Bone SPECT/CT in Oncology

8

Kanhaiyalal Agrawal and Gopinath Gnanasegaran

8.1 Introduction

Bone scintigraphy is a routine nuclear medicine procedure mainly used to detect bone metastases in a cancer patient. Bone scintigraphy has traditionally been the mainstay of whole-body screening for bone metastases. A planar bone scan is sensitive in detecting osteoblastic bone metastasis but has limited specificity due to non-specific uptake in benign bone conditions. Almost half of the solitary focus on planar bone scintigraphy in patients with a malignancy history may be benign abnormalities. Hence, radiological correlation is necessary in some of the cases showing radiotracer uptake in bones. Hybrid SPECT/CT can provide:

- Functional and morphological data in one examination.
- Increasing the specificity of bone scintigraphy.
- Avoiding indeterminate findings and additional investigation.

8.2 Radiopharmaceutical for Bone Scintigraphy/ SPECT-CT

SPECT tracers used in bone scintigraphy are Technetium-99m (99mTc) based. The tracers are 99mTc methylene diphosphonate (99mTc MDP), 99mTc hydroxymethylene diphosphonate (99mTc HDP or HMDP), 99mTc hydroxyethylidene diphosphonate (99mTc HEDP) and 99mTc pyrophosphate.

The bone imaging agents are either phosphates or diphosphonates. The P-O-P bond in phosphate is easily broken down by phosphatase enzyme and is less stable in vivo than a stable P-C-P bond in diphosphonate. Therefore, diphosphonate is a commonly used radiopharmaceutical in bone imaging [1]. The diphosphonate agents are usually available in kit form. Labelling occurs by adding pertechnetate to the cold kit and mixing. Generally, the oxidation state of 99mTc in bone kits is 3+. The uptake in bone is due to ion exchange phenomena. 99mTc diphosphonate binding occurs by chemisorption in the hydroxyapatite mineral component of the bone matrix. Both tracers are primarily excreted through kidneys.

K. Agrawal
Department of Nuclear Medicine, All India Institute of Medical Sciences (AIIMS), Bhubaneswar, India

G. Gnanasegaran (✉)
Royal Free NHS Foundation Trust, London, UK
e-mail: gopinath.gnanasegaran@nhs.net

H. Ahmadzadehfar et al. (eds.), *Clinical Applications of SPECT-CT*,
https://doi.org/10.1007/978-3-030-65850-2_8

8.3 Radiopharmaceutical Activity

An adult's recommended activity is intravenous injection of 740–1110 MBq (20–30 mCi) of 99mTc-labelled agents. For obese patients, the administered tracer activity is increased to 11–13 MBq/kg (300–350 μCi/kg). In kids, the recommended dose is 9–11 MBq/kg (250–300 μCi/kg), with a minimum of 20–40 MBq (0.5–1.0 mCi) [2].

8.4 Bone SPECT/CT Patient Preparation

The patient preparation for bone SPECT/CT is similar to bone scintigraphy. In general, before making an appointment for bone scintigraphy and SPECT/CT, pregnancy and active breastfeeding should be ruled out in female patients. No specific patient preparation is required for bone scintigraphy. Unless contraindicated, the patient should be well hydrated before and during the study. The Nuclear medicine team should document relevant medical history related to the investigation before radiotracer administration. In particular, the referral cause, current symptoms, history of trauma or fractures, prior bone scintigraphy results, any history of allergy, renal impairment, etc., should be recorded. Past medical history of surgery, chemotherapy or radiotherapy to the patient must be documented. Any recent nuclear medicine studies which may impair bone scintigraphy image quality must be reported [3].

In between administration of tracer and study acquisition, the patient should void frequently and immediately before the scan. All metallic objects must be removed during imaging unless contraindicated. The non-removable metallic objects like pacemakers must be documented before study.

8.5 Image Acquisition Protocol

Always bone SPECT/CT is preceded by planar bone scintigraphy image acquisition. In planar whole-body imaging, anterior and posterior view images are acquired. The whole-body scan is acquired to obtain more than 1.5 million total counts. The table rate should be adjusted depending on the equipment manufacturer's specification. The energy window should be centred at 140 keV. Window width is kept at 15–20%. Matrix size is 256 × 1024 or higher. If needed, spot view may be acquired depending upon the clinical indications and should be 500K–1000K per image (less for skull and extremities). Additional three-phase acquisition, lateral, oblique or special (frog-leg views of the hips) views may be acquired if necessary.

SPECT acquisition has the following parameters: Contoured orbit, 64 × 64 or greater matrix, 3–6° intervals, 10–40 s/stop. SPECT image reconstruction is done with 3D iterative OSEM (ordered-subsets expectation-maximization) with ideally 3–5 iterations and 8–10 subsets. CT acquisition parameters are 120 kV, 30–100 mA/slice (or intensity-modulated), and slice thickness depends on the body part imaged (1.5–2 mm) [4]. Usually, a contrast medium is not necessary for SPECT-CT of bones. Literature evidence suggests that even low-dose CT protocols with low-tube current-time products in the range of 2.5–30 mAs give good diagnostic accuracy [5].

SPECT-CT is usually done with a CT field of view restricted to the equivocal or indeterminate tracer uptake seen on the planar study called SPECT-guided low-dose CT or targeted SPECT-CT. This procedure gives less extra average radiation dose to the patient (generally additional 2–3 mSv depending on CT protocol used). However, some researchers have shown better accuracy of whole-body SPECT-CT, which is discussed later in this chapter.

8.6 Role of SPECT-CT in Bone Metastases

Early and accurate detection of bone metastases is crucial for better management of cancer patients and preventing complications. The most common bone metastasis sites are the vertebral column and pelvic bones due to the high proportion of red marrow in these bones [4]. Approximately 60–80% of patients with breast and prostate cancer develop bone metas-

Table 8.1 Different responses from bone metastasis in various malignancies

Predominantly osteoblastic	Predominantly osteolytic	Mixed osteoblastic and lytic
Prostate cancer	Thyroid cancer	Breast cancer
Hodgkin lymphoma	Renal cell carcinoma	Stomach cancer
Carcinoid	Non-small cell lung cancer	Colon cancer
Small cell lung cancer	Multiple myeloma	Urinary bladder cancer
Medulloblastoma	Melanoma	Squamous cancers
	Langerhans-cell histiocytosis	

tases [6]. About 90% of patients with multiple myeloma develop osteolytic bone metastases [7]. According to the plain radiographic appearances, bone metastases are generally classified as lytic, sclerotic, or mixed. Wherever bone resorption predominates with little new bone formation, the metastases will have a lytic appearance. Table 8.1 mentions different types of responses to bone metastases in various malignancies. Literature evidence of biochemical markers of bone turnover indicates that all three types of radiological metastases are associated with biochemical evidence of increased bone turnover [8]. Complex endocrine interactions with tumour biology have led to a greater understanding of bone metastases and allowed several novel interventions for metastases and treatment-related osteoporosis [8]. Lytic lesions are particularly interesting as successful therapy leads to progressive sclerosis of the lesions [9], which in scintigraphy studies manifests as the 'flare' phenomenon [10].

8.7 Radiological Imaging

The plain film is a relatively insensitive method for evaluating bony metastatic disease in the absence of symptoms. It is crucial as a screening tool in multiple myeloma. The principal advantage of the plain film is that its findings may help to identify the primary tumour, exclude benign conditions and predict the risk of pathological fracture, mostly if more than 50% of the cortex has been destroyed by the tumour [11].

While CT scanning is more sensitive than conventional radiography, it is not an appropriate investigation for screening the entire skeleton. The CT scan's great strength lies in confirming suspicious lesions that are apparent on either plain film or bone scintigraphy with clarification of the anatomic site and extent of cortical destruction.

MRI is highly sensitive for detecting skeletal metastases at a nascent level when the tumour deposits have infiltrated bone marrow. The normal fat cells in the bone marrow are displaced by tumour cells. The T1-weighted study will demonstrate low-signal intensity at infiltration sites and high-signal intensity on fat-suppressed images. Metastases also have a bright T2 signal around them [11]. Diffusion-weighted whole-body MRI has shown similar sensitivity to skeletal scintigraphy in detecting metastases from prostate, breast cancer or non-small cell cancer of the lung [12, 13].

8.8 Bone Scintigraphy

Bone scintigraphy detects bone metastases when there is a reactive increase in bone formation. The advantage of bone scintigraphy is screening the entire skeleton with extremely high sensitivity for detecting metastases, particularly in prostate and breast cancer. Literature evidence demonstrated that bone scan sensitivity in detecting metastases is 85–96% [14–16]. However, the diagnostic accuracy of planar and SPECT bone scintigraphy is limited due to the non-specific nature of radiopharmaceutical in bone disease and relatively poor spatial resolution. The specificity of bone scintigraphy in detecting bone metastases is low because many benign bone diseases show abnormal radiotracer accumulation leading to false-positive diagnosis (Table 8.2) [17]. However, SPECT/CT leads to characterization of tracer uptake leading to improved bone scintigraphy specificity.

Further, the lesion may be missed if it is tiny in size on planar bone scan [18]. Planar bone

Table 8.2 Metastatic patterns on planar bone scintigraphy

Metastasis	Benign uptake mimicking metastasis
• Randomly scattered multifocal uptake • Diffuse heterogeneous uptake in skeleton • A cold defect with peripheral rim uptake (lytic lesion) • Photopenic defect • Asymmetric uptake in growth plates of long bones in children in neuroblastoma	• Multifocal uptake in contiguous ribs could be post-traumatic • Multifocal uptake may be seen in polyostotic bone dysplasia • Multifocal uptake in the facet joints/endplate region of spine could be degenerative changes • Diffuse uptake in the long bones due to hypertrophic pulmonary osteoarthropathy

Table 8.3 Advantages and disadvantages of bone SPECT-CT

Advantages	Disadvantages
1. Provides both anatomical and functional data in one study, therefore increasing the sensitivity and specificity of the planar study	1. Increase in radiation burden to patient
2. Avoiding additional investigation due to equivocal findings in planar study, which could be time consuming and uncomfortable for the patient and also leads to delay in diagnosis	2. Increase in scan time leading to patient discomfort and decrease in output of the department
3. Attenuation correction by CT data	3. Expensive equipment
4. Incremental value due to incidental findings	4. Non-uniform protocols

scintigraphy has low sensitivity in detecting purely lytic lesions seen in renal cancer, lymphoma and breast cancer. CT component of the SPECT/CT helps detect small and lytic lesions, increasing the sensitivity of the investigation.

8.9 Bone SPECT-CT

SPECT-CT helps increase the planar bone scintigraphy's sensitivity by detecting tracer non-avid lytic lesions or small lesions missed on planar study. The specificity of planar and SPECT study is augmented by accurate localization and characterization of the tracer uptake by SPECT-CT. Moreover, in the staging of disease, the leading utility of SPECT-CT lies in differentiating degenerative disease in the spine common in the elderly patient from metastatic disease. For this purpose, localization of tracer uptake with low-dose CT protocol is sufficient for accurate differentiation of nature of uptake. The advantages and disadvantages of SPECT-CT in bone metastases are mentioned in Table 8.3.

8.10 Artifacts on SPECT/CT

There are different types of image artifacts on SPECT/CT, as mentioned in Table 8.4 [19].

8.11 Literature Evidence on the Role of Bone SPECT/CT in Metastases

There is published literature evaluating SPECT/CT's role in detecting bone metastases in indeterminate or equivocal lesions on planar bone scans. A meta-analysis studying the role of SPECT/CT in classifying indeterminate bone lesions on planar bone scintigraphy, the pooled sensitivity and specificity of SPECT/CT was reported as 93% [95% confidence interval (CI) 0.91–0.95] and 96% [95% CI 0.94–0.97], respectively [20]. The summary of the articles is mentioned in Tables 8.5 and 8.6. SPECT/CT characterizes most of the equivocal findings on planar bone scan with acceptable accuracy in all the studies. SPECT/CT's sensitivity and specificity were found better than planar and SPECT

Table 8.4 Artifacts in SPECT-CT

Artifacts	Effect on image quality
Artifacts on CT component	
• Motion during CT acquisition	Blurring of the contours, disturbances in whole image
• Beam hardening artifacts (Fig. 8.1)	Streaks between bone structures
• Partial volume effects due to structures which are only partially included in the slice	Dark and light streak artifacts
Artifacts on SPECT-CT	
• Misregistration due to poor calibration of isocentres, patient movement (Fig. 8.2a–c)	Wrong localization of tracer uptake leading to misinterpretation, wrong attenuation correction leading to false visualization of uptake
• Truncation artifacts if field of view is too small or patient is too large or patient arm is extended outside selected field of view (Fig. 8.1)	Leads to streak artifacts and hyperdense areas on CT
• High attenuation foreign bodies, e.g. metal artifacts, CT contrast agent, barium (Fig. 8.3)	Leads to low photon counts and high noise, streak artifacts and inaccurate attenuation coefficient measurement
• CT noise due to large patient or low-dose CT protocol (Fig. 8.4)	Low photon counts, error in defining of the CT numbers, loss of smaller details

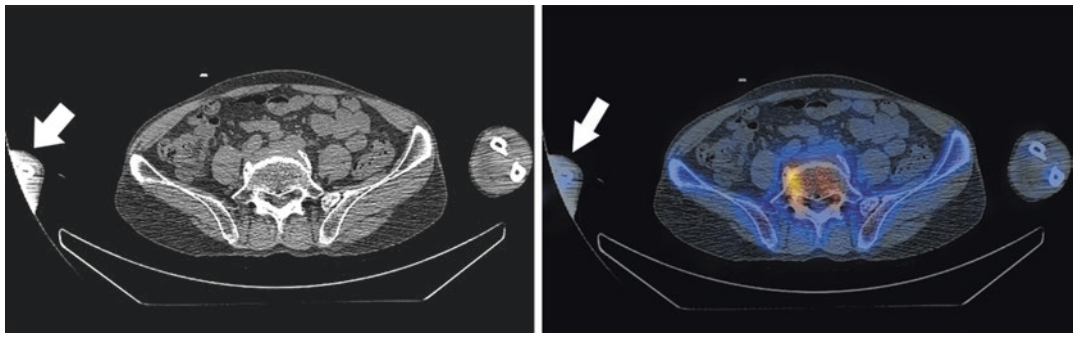

Fig. 8.1 Truncation artifact on CT leading to hyperdense area in the region of right forearm bones (arrow) and streak artifacts due to truncation as well as beam hardening

bone scintigraphy to detect metastases in almost all research.

A new perspective for bone SPECT/CT is whole-body SPECT/CT rather than targeted SPECT/CT. Some studies have shown higher sensitivity, but similar specificity to one-field-of-view targeted SPECT/CT [33]. However, there is a marginal incremental diagnostic value for whole-body SPECT/CT compared to one-field-of-view SPECT/CT [34]. With the availability of faster acquisition protocols for SPECT/CT, whole-body bone SPECT/CT could be widely used [35].

Different scenarios where bone SPECT/CT is contributary in bone metastases evaluation.

(a) Differentiation of degenerative bone diseases/fracture from metastases:

SPECT/CT localizes and characterizes the abnormal tracer uptake leading to differentiation of degenerative changes, facetal arthropathies, enthesopathies, fractures and osteoporotic collapse from metastases (Figs. 8.5, 8.6, 8.7, 8.8, 8.9, 8.10, 8.11, 8.12, and 8.13), and this is the most common use of bone SPECT/CT in oncology.

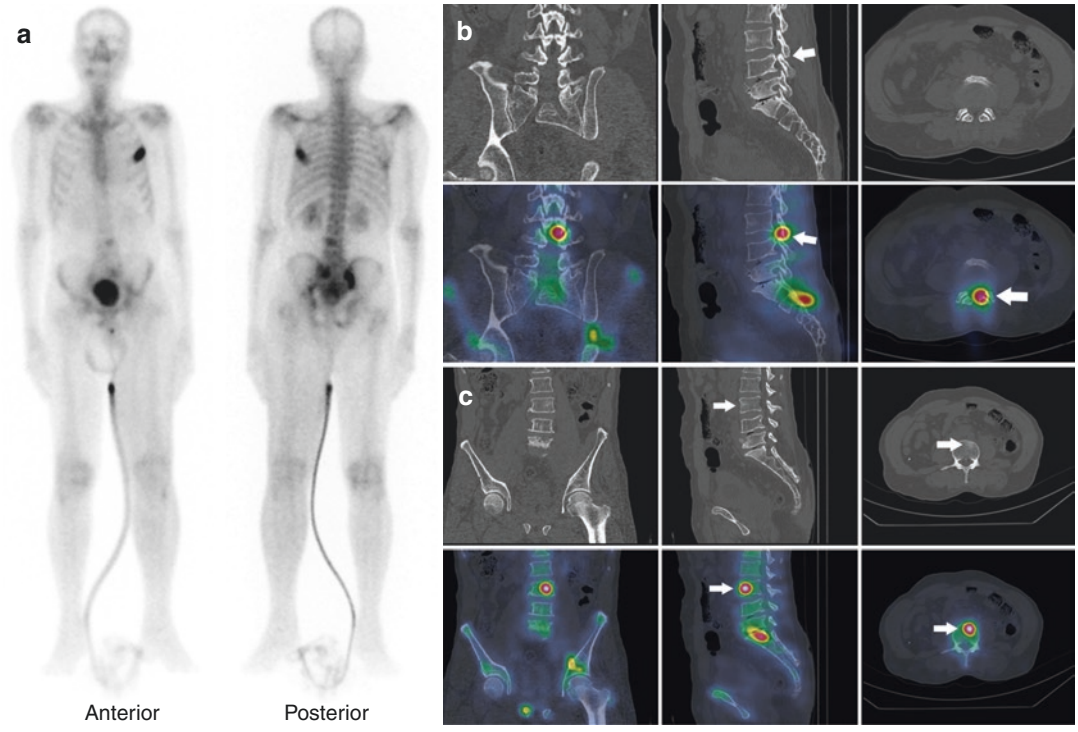

Fig. 8.2 (**a**–**c**) Misregistration: Known carcinoma prostate, whole-body bone scan (**a**) shows multifocal uptake in the left rib, lower lumbar spine and pelvic bones. SPECT/CT of the lumbar spine and pelvis (**b**) localizes the uptake in the lumbar region to the left L3–L4 facet joint (arrow); however, fused coronal image shows gross misregistration between CT and SPECT images. On inquiry, the technologist informed that patient moved during image acquisition. However, as some anatomical landmarks were available, manual registration of images localizes the uptake to the L3 vertebral body (arrow) and sacrum showing minimal sclerosis (**c**) suggestive of metastasis

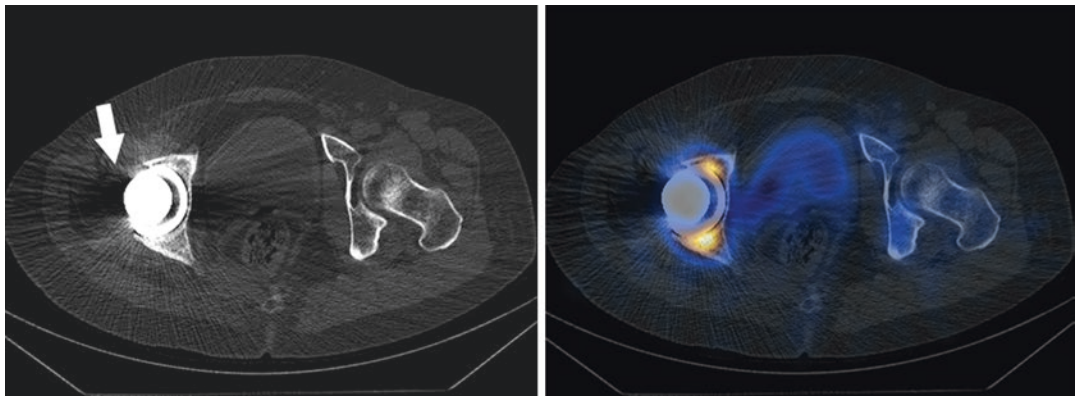

Fig. 8.3 Metal artifact due to hip prosthesis shows darkening adjacent to the metal and streak artifact leading to poor image quality

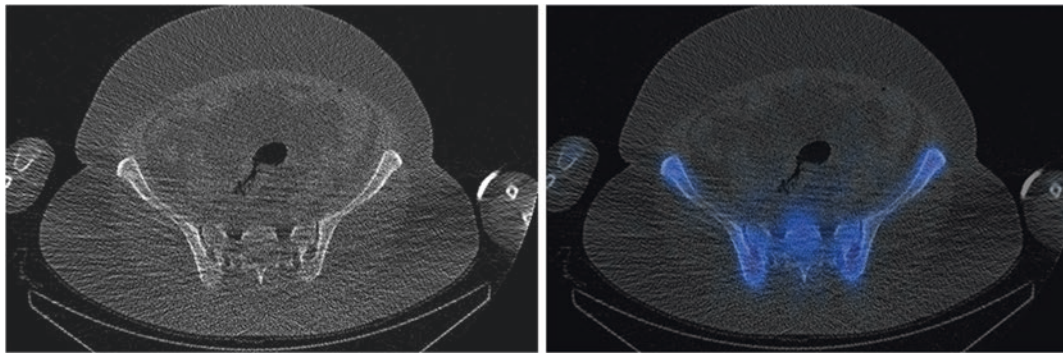

Fig. 8.4 Low-dose CT protocol with 10 mAs and 120 kV in an obese patient leading to high noise and poor image quality

(b) Differentiation of benign bone diseases from metastases:

Several benign bone diseases mimic metastases on planar bone scintigraphy, e.g. Paget's disease (Fig. 8.14), fibrous dysplasia, exostosis, haemangioma (Fig. 8.15), hypertrophic osteoarthropathy. Although some of these entities produce typical appearance on planar bone scintigraphy, other correlative anatomical imaging is required. SPECT/CT acts as one-stop-shop imaging for differentiation of these benign bone entities from metastases.

(c) Extra-skeletal uptake:

There could be extra-skeletal uptake of radiotracer in a bone scan which may mimic bone uptake. Transplant and ectopic pelvic kidney may resemble abnormal uptake in the pelvic bones (Fig. 8.16). Non-osseous tracer uptake is seen in splenic infarct, liver metastasis (Fig. 8.17), lung metastasis (Fig. 8.18), ascites (Fig. 8.19), urinary bladder stones, physiological bowel uptake (Fig. 8.20), etc. Sometimes, the primary tumour shows tracer uptake and should be differentiated from metastases, e.g. neuroblastoma primary, lung cancer, soft-tissue Ewing sarcoma (Fig. 8.21).

(d) Differentiation of local bone infiltration of primary from metastases:

The uptake in the bone could be due to primary local infiltration or secondaries in the bone. This dilemma often occurs if the uptake is seen in a bone close to the primary site. SPECT/CT is usually helpful in this scenario (Fig. 8.22). Differentiation of local infiltration from metastatic bone involvement leads to change in management.

(e) Lytic metastases and metabolically inactive disease:

A planar bone scan has lower sensitivity in the detection of lytic bone metastasis. CT component of the SPECT/CT detects the small lytic lesions, hence increasing the bone scan's sensitivity (Figs. 8.23 and 8.24). Further, SPECT, due to increasing spatial resolution, may detect mildly increased tracer uptake due to bone reaction secondary to lytic metastases not seen on planar scintigraphy. Some authors suggest that the areas that cause pain and a high likelihood of metastases should be included in SPECT/CT, even if planar bone scintigraphy is negative [36]. Sometimes, the sclerotic lesions may not show tracer uptake or show very low-grade uptake on planar study if the patient is on treatment, where SPECT/CT increases the diagnostic sensitivity (Figs. 8.25 and 8.26).

(f) Prognostication value:

The abnormally increased tracer uptake on bone scintigraphy could be due to pure sclerotic or mixed lytic sclerotic metastases [36]. However, both have different prognos-

Table 8.5 Studies evaluating role of SPECT/CT in indeterminate bone lesions on planar bone scan—lesion-based evaluation

Author (year)	Number of patients included in study	Study design	Radiotracer used	Parts of body SPECT-CT	CT used in SPECT-CT	CT radiation dose mAs and kV	Sensitivity (%)	Specificity (%)	Comment
Gayed et al. (2011) [21]	19	Retrospective	MDP	Targeted	6 slice	90, 130	100	92	Evaluation of solitary skull lesions
Sharma et al. (2012) [22]	50	Retrospective	MDP	Targeted	6 slice	100, 130	96 and 98[a]	89	Only lung cancer patients
Sharma et al. (2012) [23]	102	Retrospective	MDP	Targeted	6 slice	100, 130	83	98	Only breast cancer patients, improvement mostly in lytic lesion
Sharma et al. (2014) [24]	32	Retrospective	MDP	Targeted	6 slice	100, 130	95	100	SPECT-CT in isolated skull uptake on bone scan (1–2 lesions) in underlying malignancy patient
Rager et al. (2018) [25]	19	Retrospective	HDP	Whole body	6 slice	40 with intensity modulation, 110	86	96	Breast cancer patient
Zhang et al. (2020) [26]	120	Retrospective	MDP	Targeted	16 slice	Not reported	100	42 and 58[a]	

[a]By two reviewers

Table 8.6 Studies evaluating role of SPECT/CT in indeterminate bone lesions on planar bone scan—patient-based evaluation

Author (year)	Number of patients included in study	Study design	Radiotracer used	Parts of body SPECT-CT	CT used in SPECT-CT	CT radiation dose in mAs (kV)	Sensitivity (%)	Specificity (%)	Comments
Palmedo et al. (2014) [27]	308	Prospective	MDP	Whole body	4 and 2 slice	2.5–20, 120	97	94	Only breast and prostate cancer patients
Fonager et al. (2017) [28]	37	Prospective	MDP/HDP	Whole body	2 and 16 slice	30–100, 130	89	100	In high-risk prostate cancer patient
Teyateeti et al. (2017) [29]	80	Prospective	MDP	Whole body	4 and 16 slice	20, 120	97	100	
Fleury et al. (2018) [30]	328	Retrospective	HMDP	Trunk SPECT-CT	2 and 16 slice	Modulation mA, 130–140	100	97	Breast and prostate cancer patients
Mavriopoulou et al. (2018) [31]	257	Prospective	HDP	Whole body	1 and 4 slice	2.5, 140	97	87.5	Breast cancer patient
Rager et al. (2018) [25]	19	Retrospective	HDP	Whole body	6 slice	40 with intensity modulation, 110	92	100	Breast cancer patient
Leiris et al. (2020) [32]	115	Retrospective	MDP	Whole body	2 slice	Not reported, 130	87	99	Prostate cancer patients

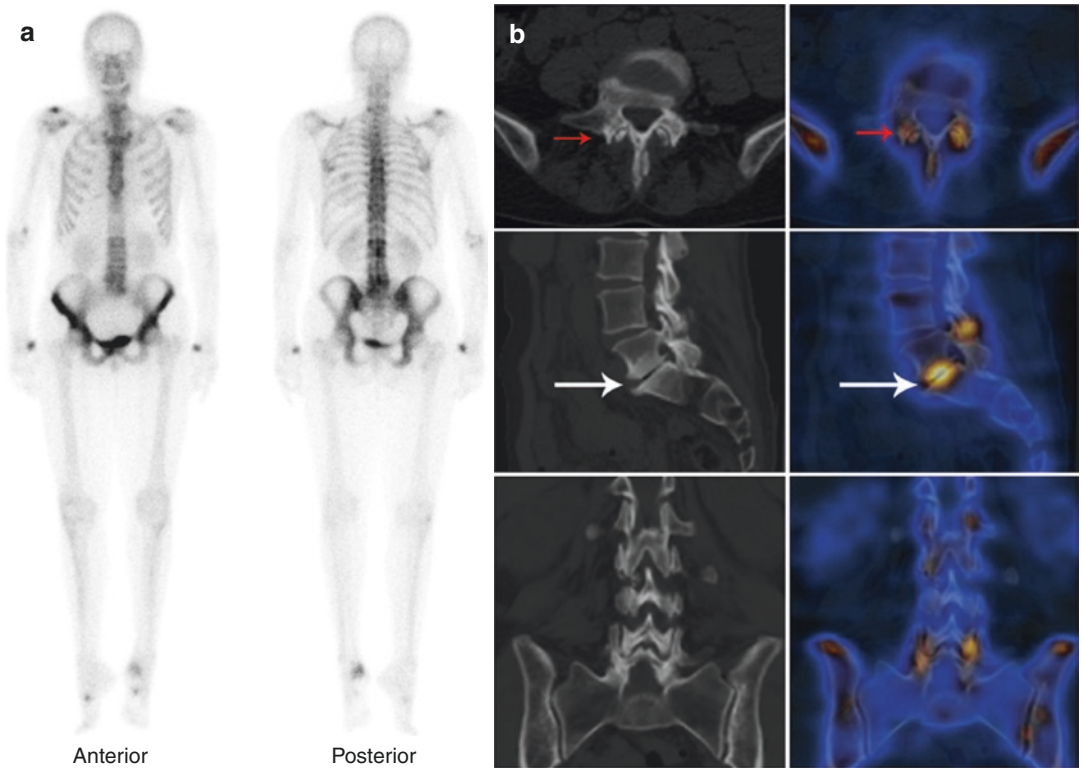

Fig. 8.5 (**a**, **b**) Lung carcinoma with diffuse heterogeneous uptake of tracer in the thoraco-lumbar vertebrae on whole-body bone scan (**a**) could be metastatic involvement. However, SPECT/CT (**b**) localizes the tracer uptake to degenerative changes in the facet joints (red arrow) and endplate changes (white arrow), therefore ruling out metastatic involvement

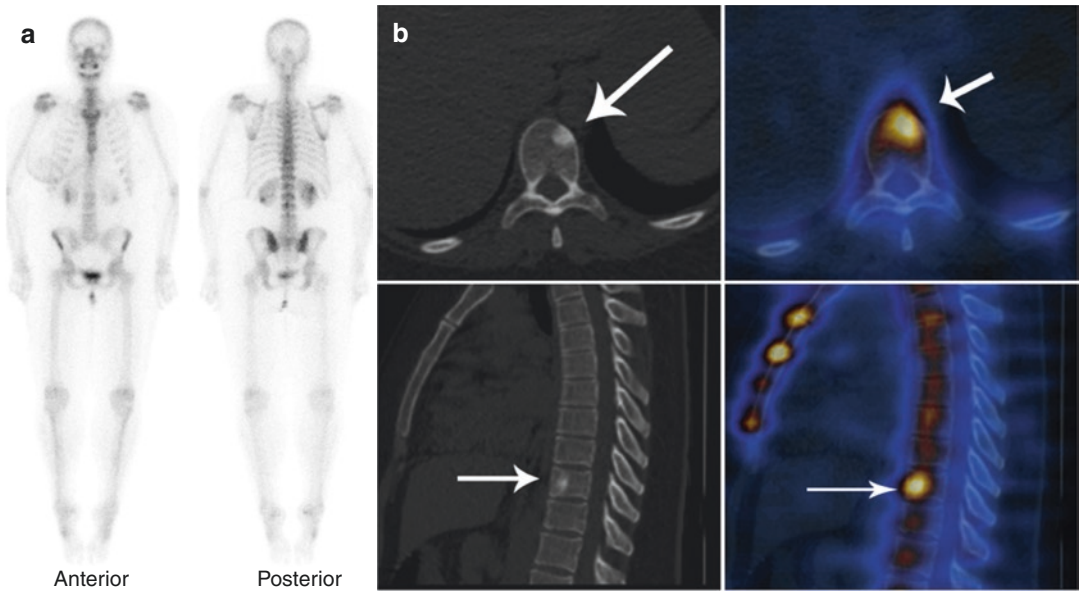

Fig. 8.6 (**a**, **b**) Breast cancer post-neoadjuvant chemotherapy. Whole-body bone scan (**a**) shows mild focal uptake of tracer in the D10 vertebra. Only planar imaging findings could be misinterpreted as degenerative changes. However, SPECT-CT of spine (**b**) localizes the uptake in the D10 vertebra to a sclerotic lesion, consistent with metastatic disease. Teaching point: SPECT-CT increases sensitivity of bone scan in determination of metastasis

tic values. Literature evidence suggests that lytic bone lesions have a relatively worse prognosis. SPECT/CT confirms the metastatic involvement of bone and classifies the lesions as pure sclerotic or mixed sclerotic-lytic, which is not always possible on planar scintigraphy due to lack of anatomical data. Further, SPECT/CT's CT component helps in detecting additional complications like impending fracture, spinal cord involvement and vertebral collapse.

(g) Increases diagnostic confidence:

Sometimes, tracer uptake is seen on the planar bone scintigraphy is confused with surface contamination of tracer (Fig. 8.27). Although cleaning the area with water and reimaging is standard protocol in suspected surface contamination, the uptake persists, leading to a diagnostic dilemma. SPECT/CT often clarifies the difficulty with certainty. Conversely, surface contamination in atypical location could be misinterpreted as sinister pathology, and SPECT/CT helps in the accurate image interpretation (Fig. 8.28). Further, in many other conditions, the SPECT/CT increases the diagnostic confidence of the reader (Figs. 8.29, 8.30, and 8.31).

(h) Incidental findings:

There could be incidental findings on a SPECT/CT performed to clarify equivocal uptake on planar bone scintigraphy. These findings might be unknown and incidentally detected, impacting patient management, e.g. detection of an ectopic kidney, soft-tissue metastases (Figs. 8.17 and 8.18), lung nodules (Fig. 8.32) and aortic aneurysm.

8.11.1 Primary Bone Malignancy

The role of bone scintigraphy is limited to the evaluation of primary bone malignancy. The bone sarcomas such as osteosarcoma, Ewing's sarcoma, chondrosarcoma show non-specific tracer

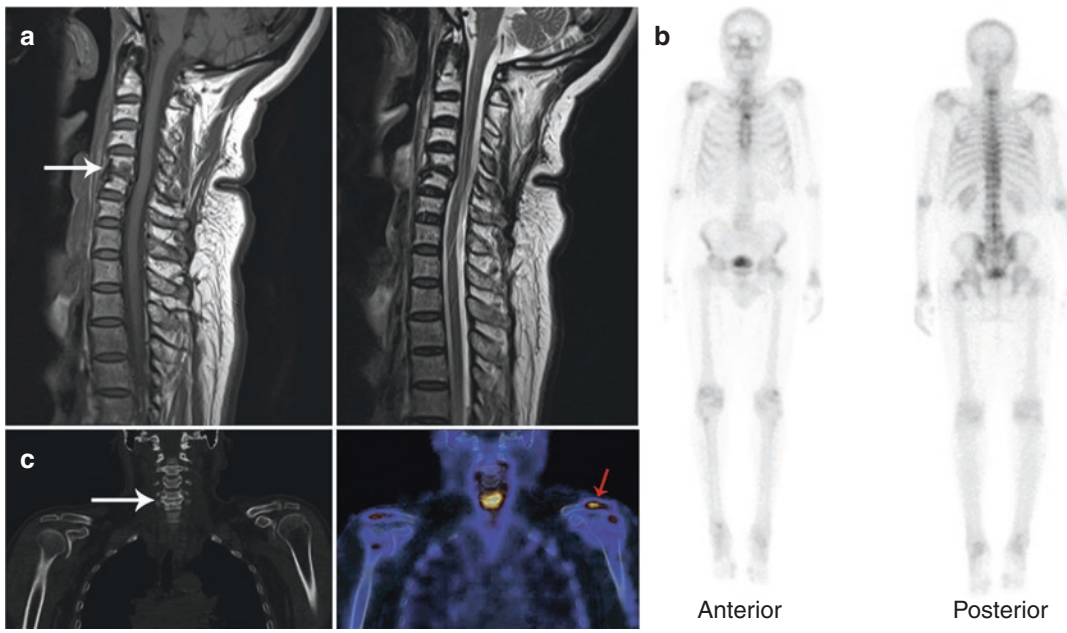

Fig. 8.7 (**a**–**c**) A patient with supraglottic carcinoma, post-radiotherapy, presented with numbness in upper and lower limbs. MRI cervical spine (**a**) shows radiotherapy changes in the C2–C6 vertebral bodies. A low-signal lesion is seen in the C5 vertebral body (arrow), likely degenerative changes. To confirm the finding and rule out metastasis, bone scan was performed. Linear tracer uptake is seen in the mid cervical spine (posterior image in **b**), which on SPECT-CT localizes to endplate degenerative changes at C5–C6 vertebrae (white arrow in **c**), thus ruling out metastatic involvement. The uptake in left acromioclavicular joint (red arrow **c**) is degenerative in nature

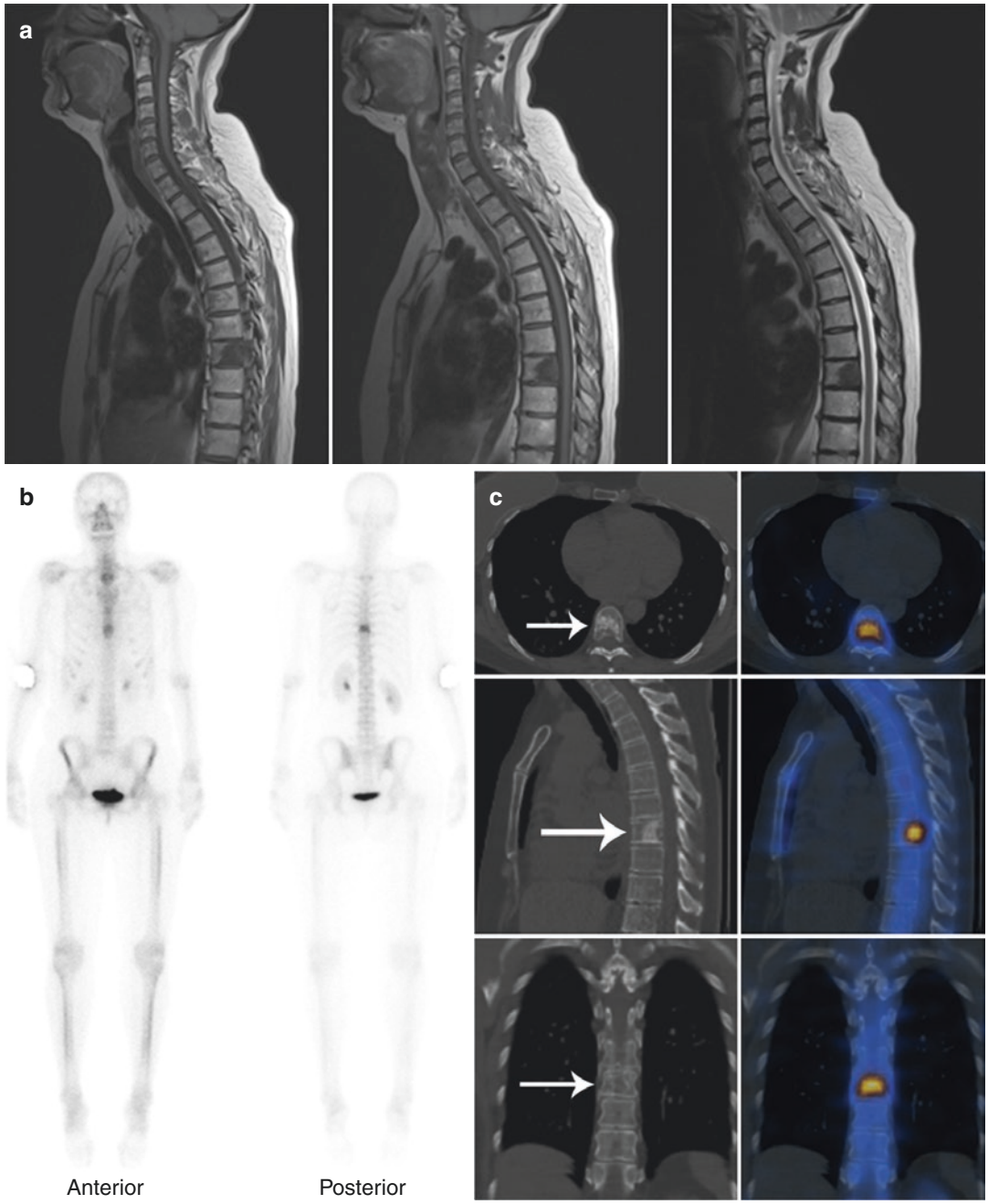

Fig. 8.8 (**a**–**c**) A 51-year-old lady with known breast carcinoma, status post-mastectomy, presented with pain in the thoracic and lumbar vertebrae, worse at night. (**a**) MR images of spine (T1, T2 and STIR sagittal sequences) show low-signal intensity lesion in the D8 vertebral body, which raises possibility of a metastasis. (**b**) Whole-body bone scan shows focal increased tracer uptake in the D8 vertebra. (**c**) SPECT-CT of thoracic spine localizes the abnormal tracer uptake seen in whole-body study to a sclerotic lesion in the D8 vertebral body (arrows), compatible with solitary bone metastasis

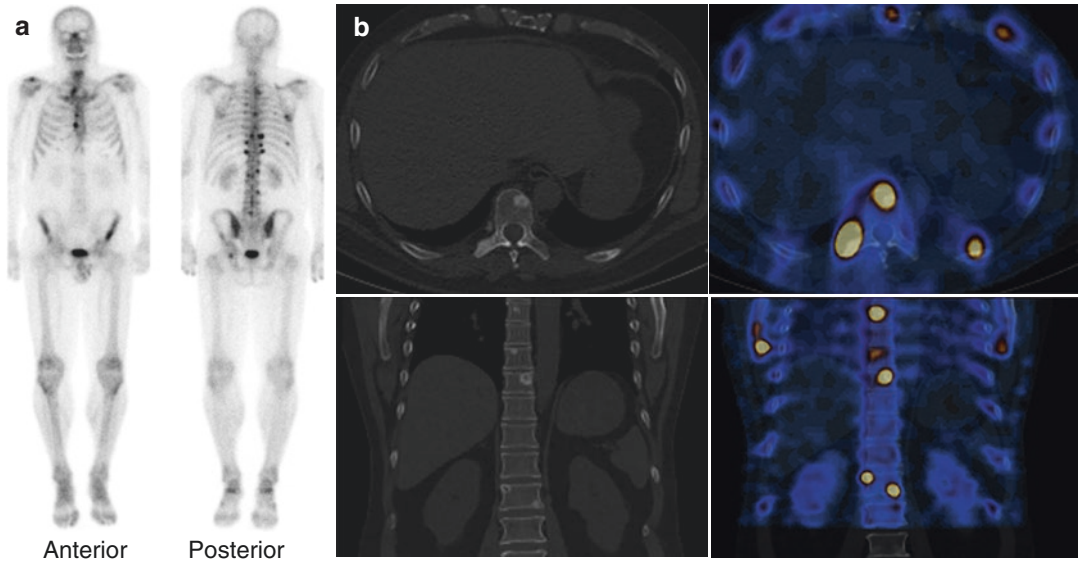

Fig. 8.9 (**a**, **b**) Prostate carcinoma with PSA level 108 ng/mL. The whole-body bone scan (**a**) shows increased tracer uptake along multiple costovertebral junctions, which could be due to degenerative changes. Similarly, low-grade uptake in the ribs could be traumatic fracture as seen in previous case. There is focal tracer uptake in the sternum and left hip joint, which are indeterminate. SPECT-CT of thorax (**b**) shows multiple sclerotic lesions in the thoraco-lumbar vertebrae involving the body and transverse process. There is also sclerotic lesion in the rib showing increased uptake of tracer. The findings are consistent with multifocal skeletal metastases

uptake on bone scintigraphy. SPECT-CT is helpful in the diagnosis of primary, mostly due to the CT component characterizing the lesion type.

However, the planar bone scan tends to overestimate the tumour extent in these tumours (Fig. 8.33). Often, SPECT-CT helps in the estimation of the accurate extent of the disease (Fig. 8.33). Whole-body bone scintigraphy has a role in detecting skip lesions in osteosarcoma and detecting osseous metastases in polyostotic tumour.

A bone scan has limited sensitivity in multiple myeloma and histiocytosis. Multiple myeloma shows lytic lesions with a lack of reactive osteoblastic reaction, so it may not be visible on a planar bone scan. Similarly, in leukaemia and lymphoma, the bone scan has limited utility. There may be increased focal uptake in the marrow in patients with marrow infiltration; however, diffuse increased osteoblastic activity may be seen in patients with blast crises.

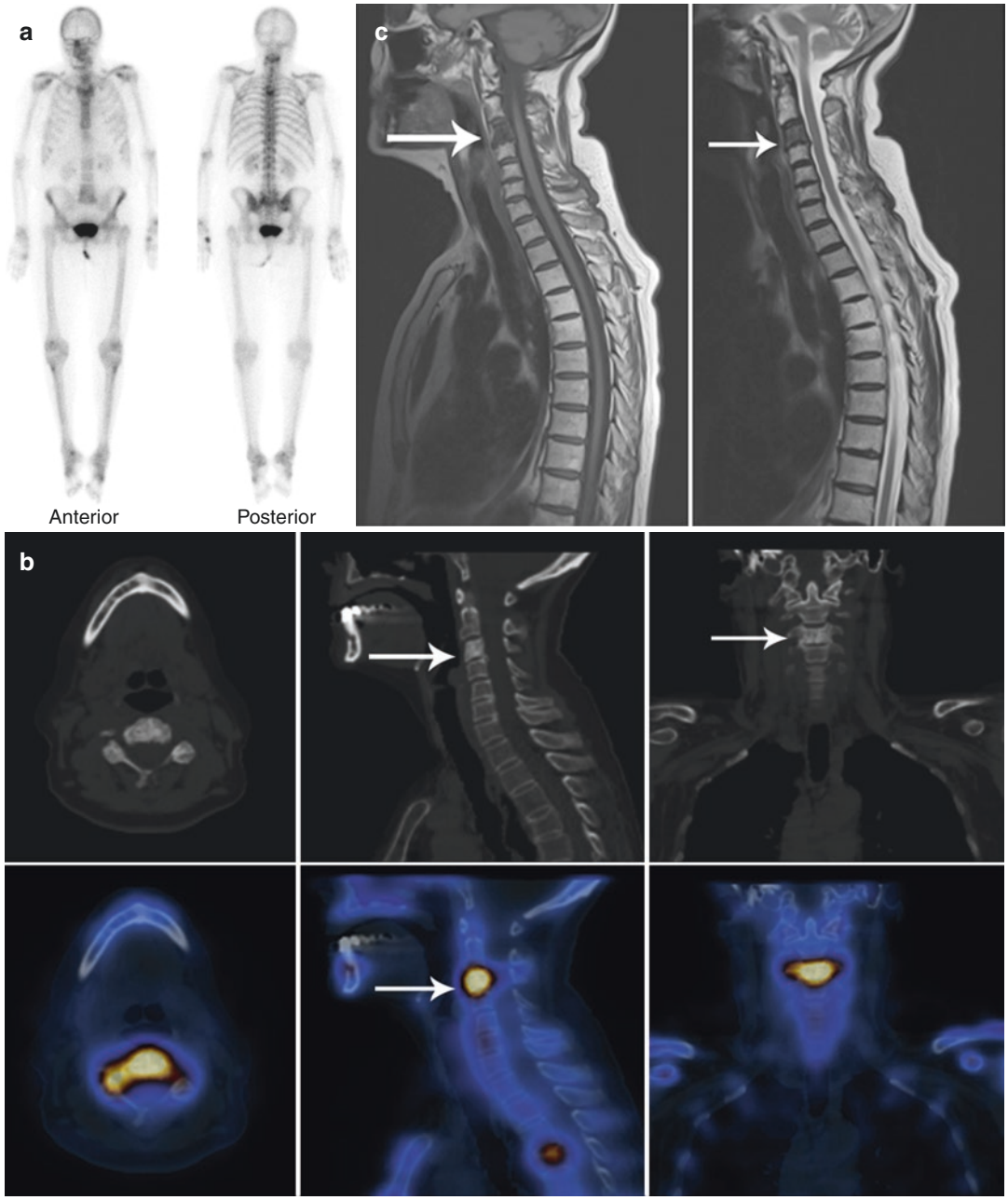

Fig. 8.10 (**a**–**c**) Lung cancer treated with radical radiotherapy and radiofrequency ablation. PET-CT scan showed uptake in C3 vertebra? which was indeterminate. Whole-body bone scan (**a**) shows mild heterogeneous tracer uptake in the upper cervical region, D4 vertebra, left lumbosacral region and right sacroiliac joint. SPECT-CT of cervical spine (**b**) localizes uptake in the cervical region to a sclerotic C3 vertebra and extends from the vertebral body into both lateral masses (arrows). The uptake in D4 vertebra localizes to partial collapse, which is new comparison to PET-CT study, morphologically favouring osteoporotic collapse. Overall, the findings are suggestive of malignant infiltration of C3 vertebra. This finding was supported by MRI cervical spine done after few days, which shows diffuse low T1-weighted and T2-weighted signal change within C3 vertebra (arrow in **c**)

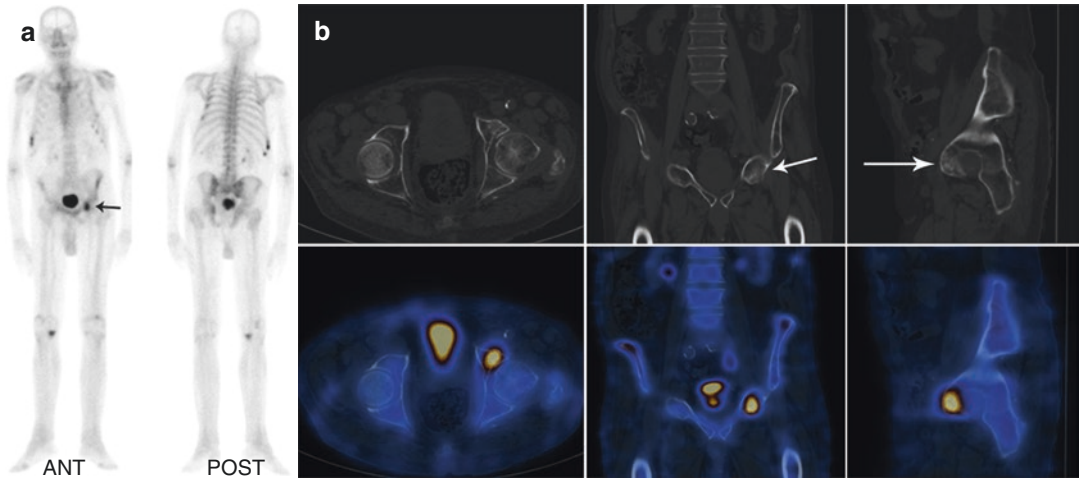

Fig. 8.11 (**a**, **b**) Patient with prostate cancer. Whole-body bone scan (**a**) shows multiple foci of increased tracer uptake in the left 6th–8th ribs and right 9th–11th ribs which are likely due to fractures. There is intense uptake of tracer in the left hip joint region (arrow). This could be due to metastatic disease. However, SPECT-CT of pelvis (**b**) localizes the uptake of tracer to the anterior column of the left acetabulum where there is a breach of cortex (arrow) and is consistent with a fracture. The findings on SPECT-CT suggested likely insufficiency fracture in the left acetabulum as there are similar fractures in the ribs; however, MRI was suggested for further evaluation

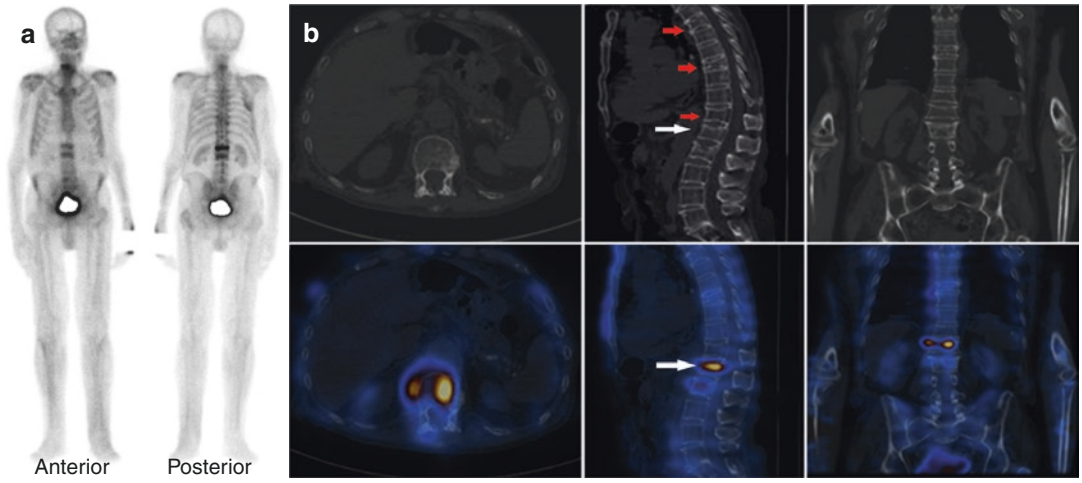

Fig. 8.12 (**a**, **b**) A 64-year-old gentleman with history of prostate cancer presented with sudden onset back pain. The patient had previous history of traumatic vertebral fracture, and exact level could not be known from the history. Bone scan was performed to identify cause of pain. Whole-body bone scan (**a**) demonstrates intense linear tracer uptake in the L1 vertebral region with more moderate linear uptake in the L2 vertebral region. Moderate tracer uptake is associated with the right aspect of the mid cervical vertebra. SPECT-CT of the thoracolumbar spine (**b**) shows marked osteoporotic changes within the thoracolumbar spine. The epicentre of the increased uptake in L1 vertebra corresponds to superior endplate of L1 where there is minor degree of endplate compression consistent with a fracture (white arrows). Mild metabolic activity in L2 is associated with more significant superior endplate compression at L2 vertebra. There are established wedge compression fractures at T6, T9 and T12 vertebrae which are metabolically inactive (red arrows). The findings are suggestive of an acute osteoporotic superior endplate compression fracture of L1 (which is likely cause of acute pain), with a previous, chronologically older compression fracture at L2

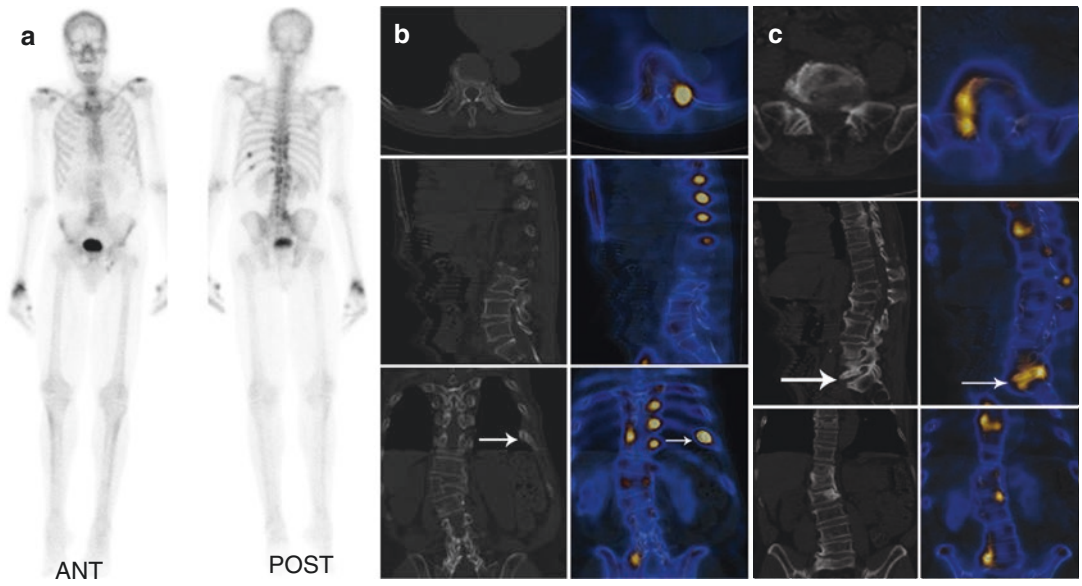

Fig. 8.13 (**a**–**c**) Prostate carcinoma with Gleason score 4 + 5 and PSA level 24 ng/mL and new onset back pain. Whole body bone scan (**a**) to look for metastatic disease shows focal tracer uptake in the left 10th and 11th ribs posteriorly, increased tracer uptake in D9–L2 vertebrae and at the right lumbosacral junction. The overall findings are suspicious for metastatic disease. There is further increased tracer uptake in the right wrist, which is likely benign in nature. However, SPECT-CT of thoracolumbar spine (**b**) localizes the tracer uptake in the left 10th and 11th ribs to site of fracture (arrow). Further, SPECT-CT of thoracolumbar spine (**b**, **c**) localizes uptake in the D9–L2 vertebrae and at right lumbosacral junction to degenerative changes (arrow in **c**). Note is also made of several collapsed vertebrae with normal tracer uptake suggestive of old traumatic/osteoporotic collapse. Overall, SPECT-CT helped in ruling out metastatic disease and identified cause of pain to be likely degenerative changes or rib fracture

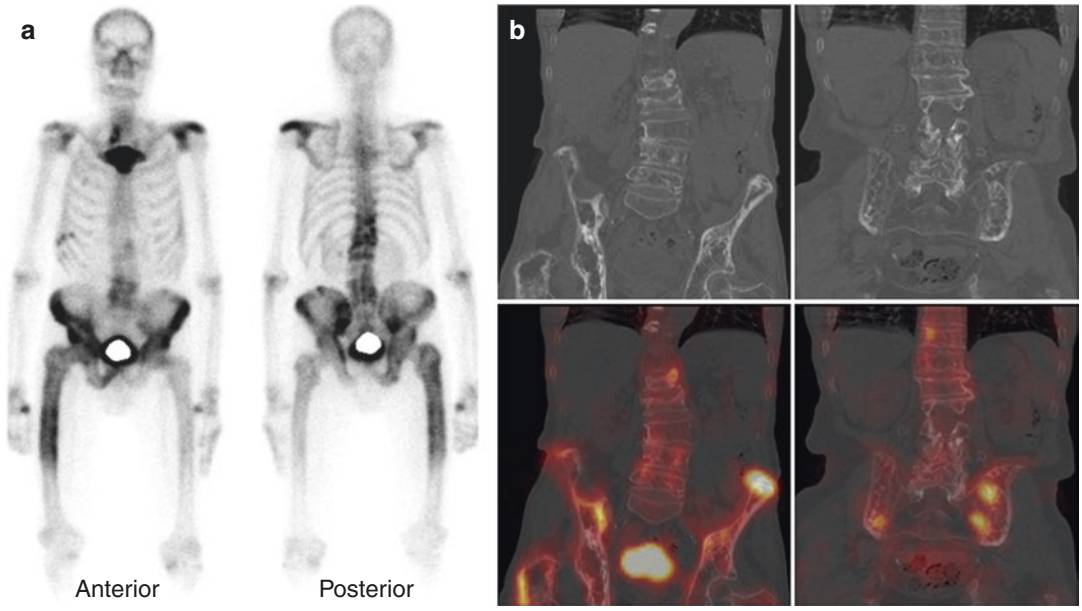

Fig. 8.14 (**a**, **b**) Bone scan was acquired from the vertex to the knees in a patient with prostate cancer. The planar bone scan shows (**a**) intense tracer uptake in the manubrium and left shoulder. Patchy tracer localization is seen in the lower thoracic and lumbar vertebrae, pelvis and bilateral femora (right side more than left). Foci of uptake in the right-side lower ribs are likely due to fractures. SPECT-CT of lower thoracic and lumbar spine and pelvis (**b**) shows marked coarsening of the trabecular pattern and cortical thickening particularly in the pelvic bones. Thus, the bone scan appearances along with SPECT-CT findings are most in keeping with extensive Paget's disease

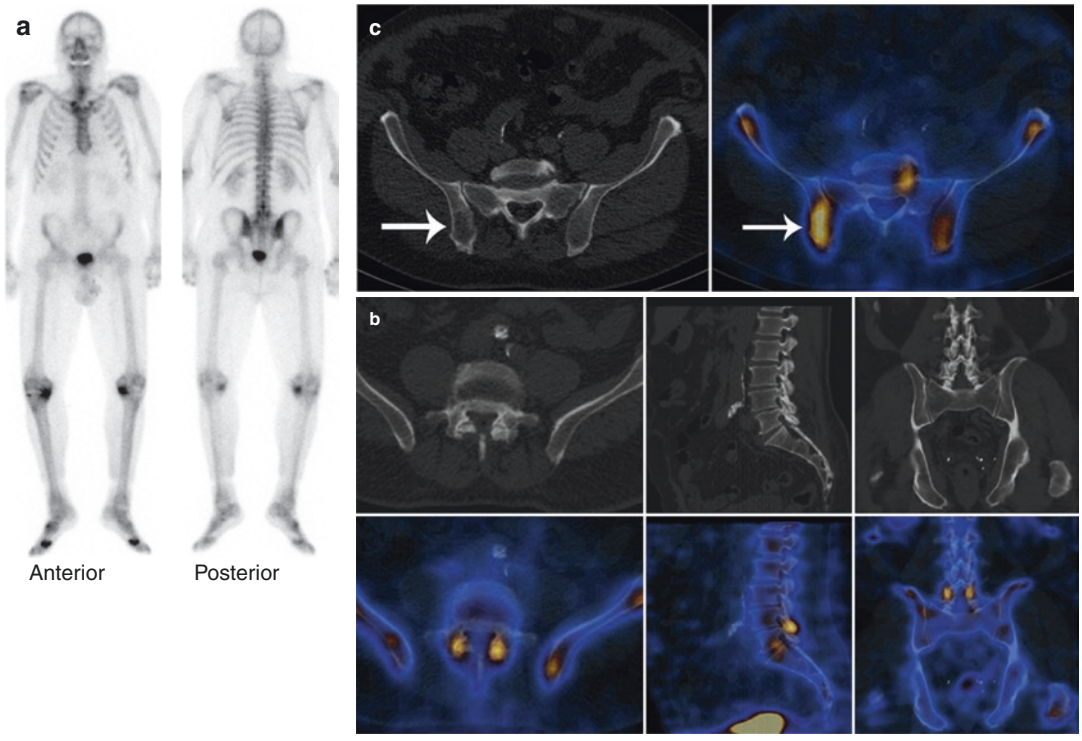

Fig. 8.15 (**a**–**c**) Patient with prostate cancer presented with 6-month history of worsening buttock pain. Whole-body bone scan (**a**) shows mild heterogeneous tracer uptake in the lower lumbar spine and right sacroiliac joint. The uptake of tracer in the knees and feet is likely due to degenerative changes. SPECT-CT of lumbar spine and pelvis (**b**) demonstrates increased tracer uptake in bilateral L4–L5 facet joints showing degenerative change on CT, which could be pain generator. Increased uptake of tracer is seen at the L5–S1 endplate changes (**b**). Further, the uptake in the right sacroiliac joint localizes to area of decreased bone attenuation in the right iliac bone (arrow in **c**). The SPECT-CT appearances of right iliac bone lesion are atypical for metastasis. MRI of pelvis showed well-defined T2 hyperintense lesion in the right ilium adjacent to the sacroiliac joint suggestive of a haemangioma (not shown)

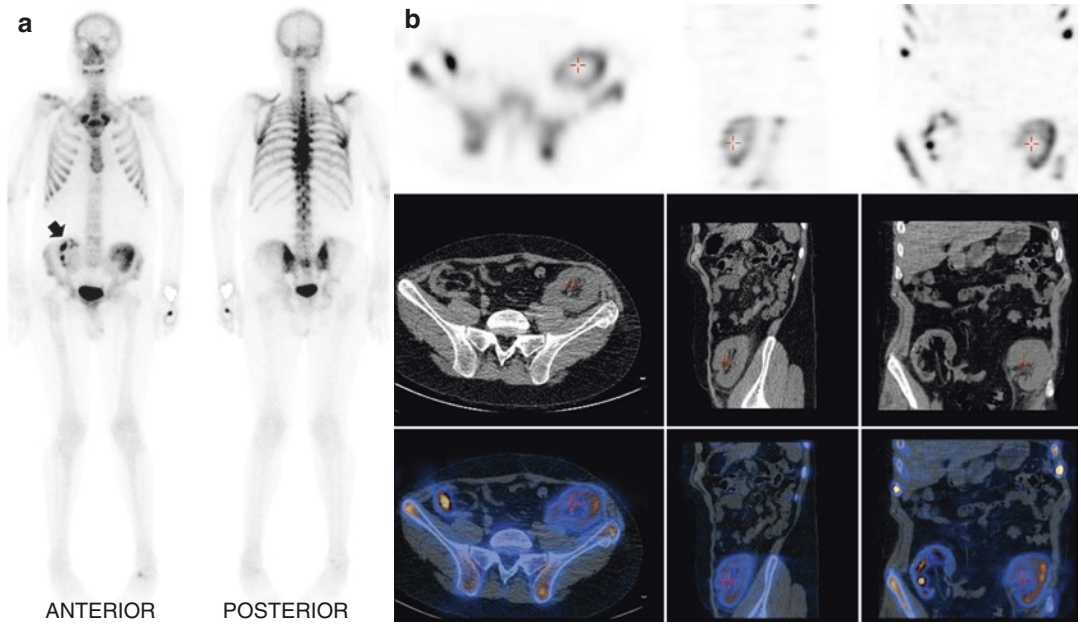

Fig. 8.16 (**a**, **b**) Patient with prostate cancer and low back pain underwent a bone scan. Whole-body bone scan (**a**) shows no abnormal tracer uptake in the lumbar spine. Abnormal tracer accumulation in the bilateral iliac fossa region in anterior image (arrow in **a**) localizes to bilateral renal transplant on SPECT-CT (**b**), suggestive of physiological tracer excretion. Heterogeneous tracer uptake in thoracic vertebrae is suggestive of degenerative changes

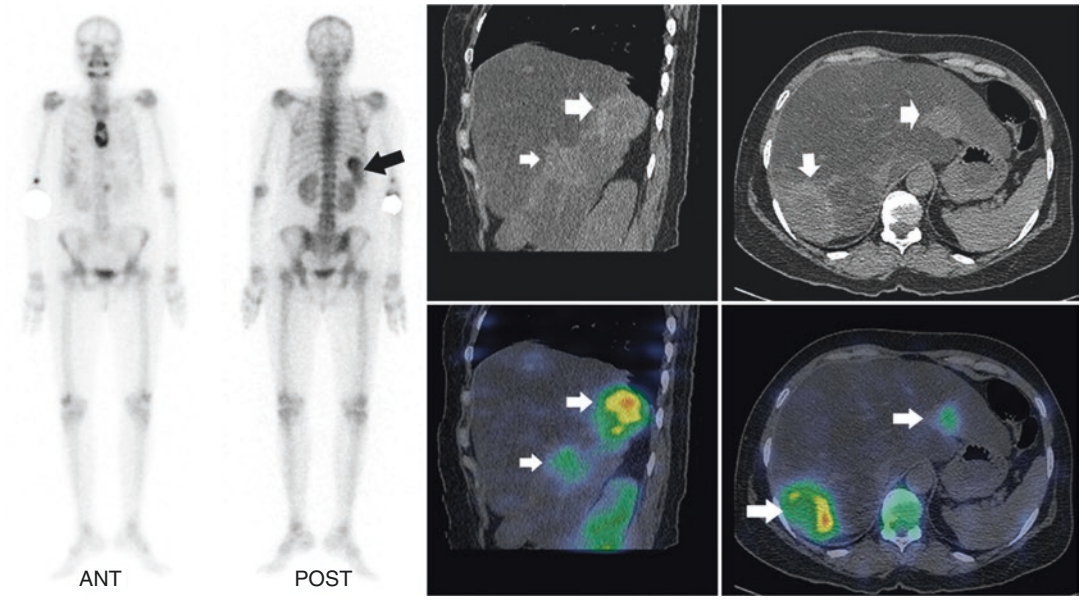

Fig. 8.17 Known carcinoma breast, whole-body bone scan shows increased uptake in the right lower thoracic region prominent on posterior view image (black arrow) as well as increased osteoblastic activity in sternum (lytic metastasis). SPECT-CT localizes the uptake in thoracic region to the hyperdense lesions in the liver (white arrows) suggestive of metastatic deposits

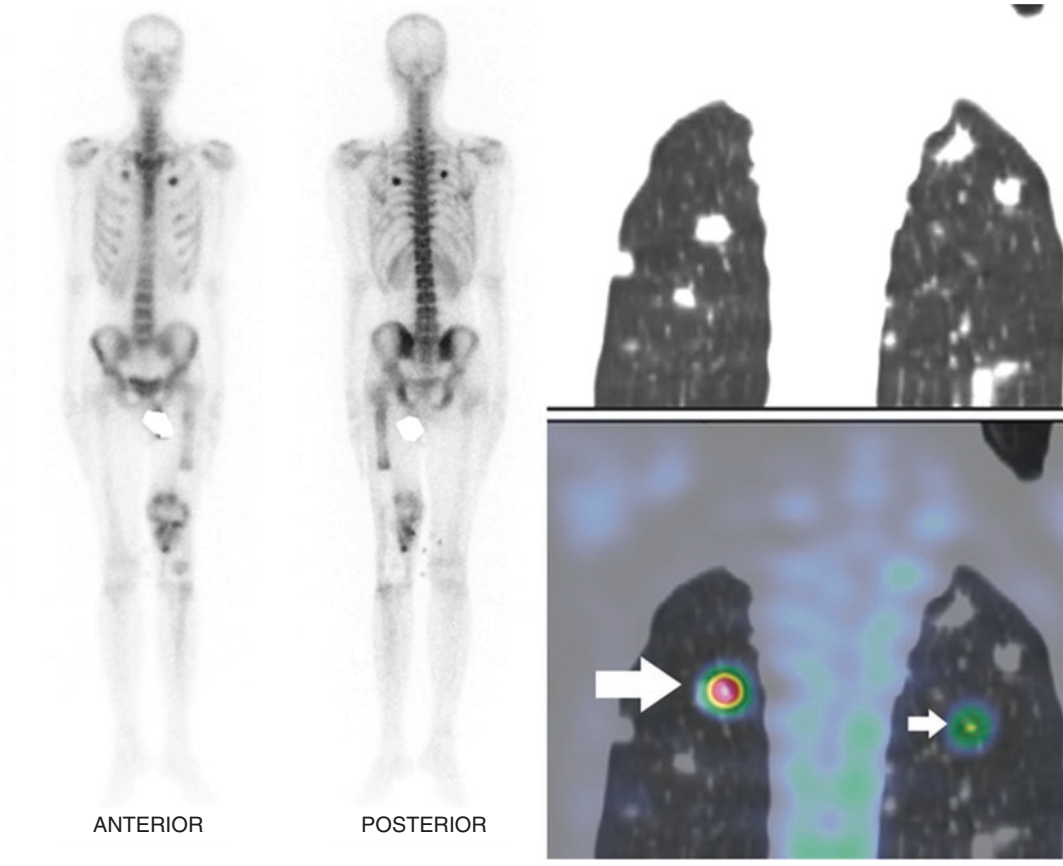

Fig. 8.18 Twenty-three-year-old male with known osteosarcoma of the left lower femur, post-surgery recurrence, bone scan shows increased heterogenous uptake at the primary site with two prominent foci of uptake in the chest could be rib metastases. However, SPECT-CT localizes the uptake to calcified lung nodules (arrows) suggestive of metastasis along with other tracer non-avid lung nodules [Teaching point: lung metastasis from osteosarcoma may show calcification leading to tracer uptake on a bone scan]

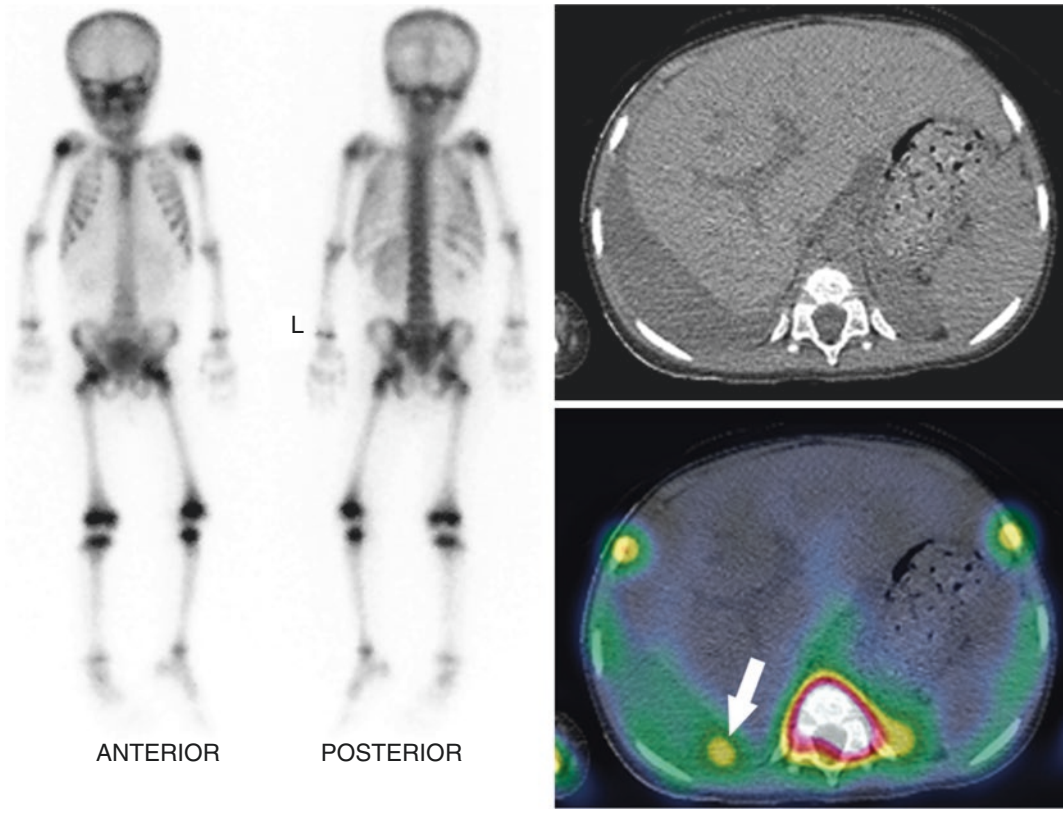

Fig. 8.19 Four-year-old boy with known Wilms tumour shows heterogeneous tracer uptake in the right lower ribs on planar bone scan, which on SPECT-CT localizes to uptake in ascitic fluid adjacent to the ribs (arrows) ruling out bone metastasis

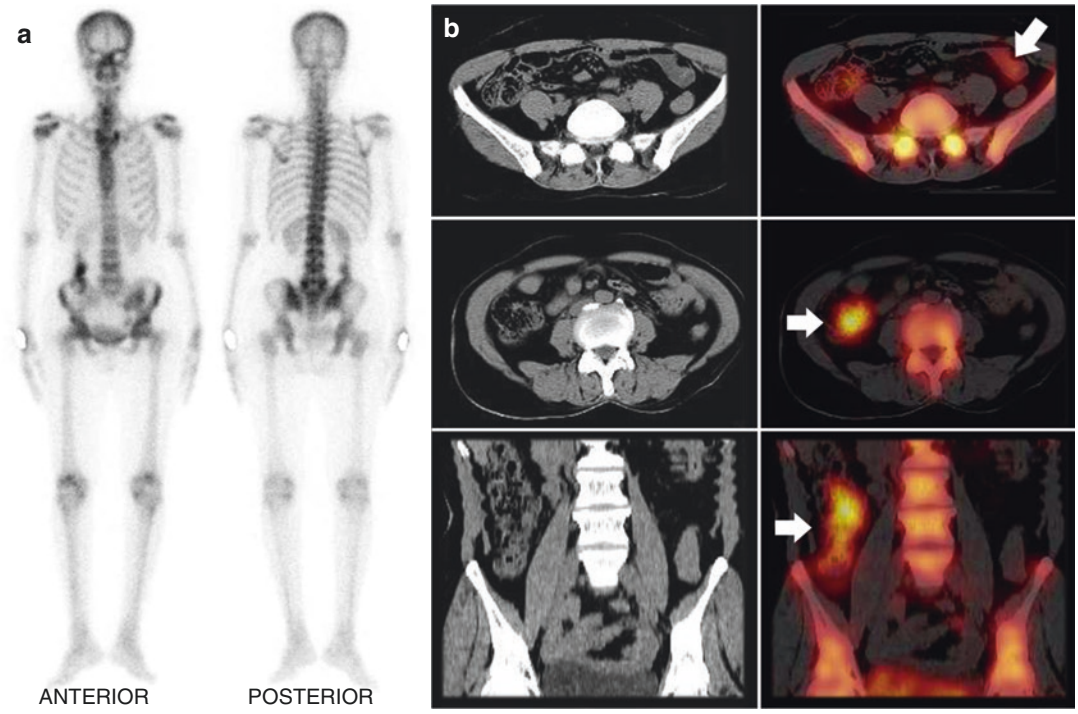

Fig. 8.20 (**a**, **b**) A patient with prostate cancer shows abnormal tracer uptake in bilateral iliac fossa on whole-body bone scan (**a**). The uptake on planar bone scan could be misinterpreted as metastasis in the left iliac bone. However, SPECT-CT of abdomen and pelvis (**b**) localizes tracer uptake in iliac fossa region to intestinal loops (arrows) suggestive of altered biodistribution of tracer. SPECT-CT helps in avoiding false-positive interpretation in cancer patient

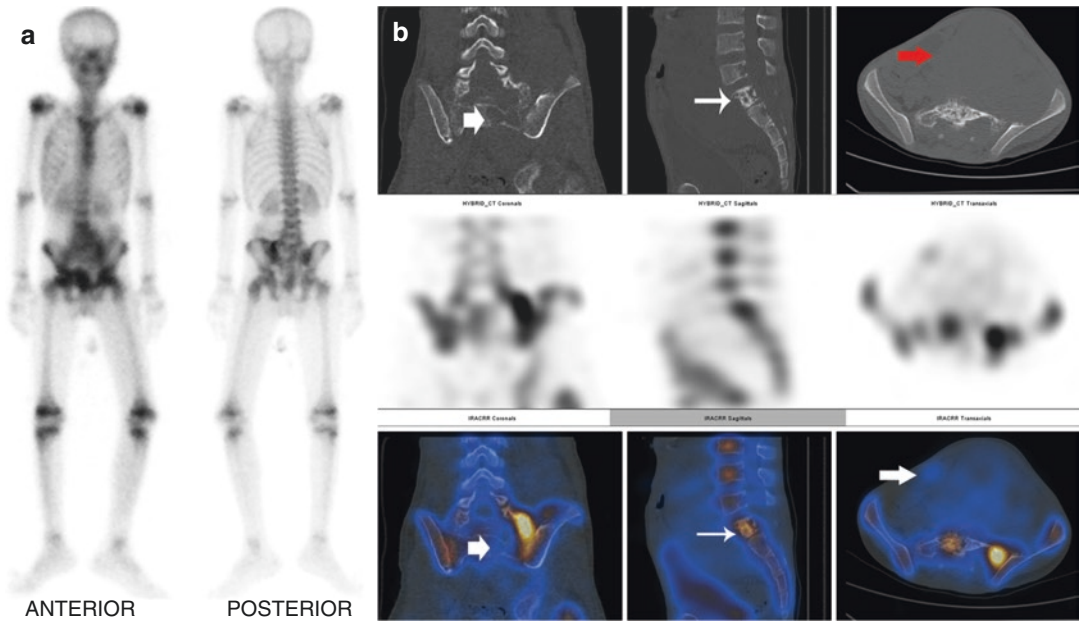

Fig. 8.21 (**a**, **b**) Known Ewing's sarcoma pelvic mass, planar bone scan (**a**) shows heterogeneous tracer uptake in the pelvis region which could be due to uptake in primary or secondary bone disease. SPECT-CT of pelvis (**b**) demonstrates uptake in the primary soft-tissue mass with uptake in the L5 and sacrum with local bone infiltration by primary mass showing lytic sclerotic lesion

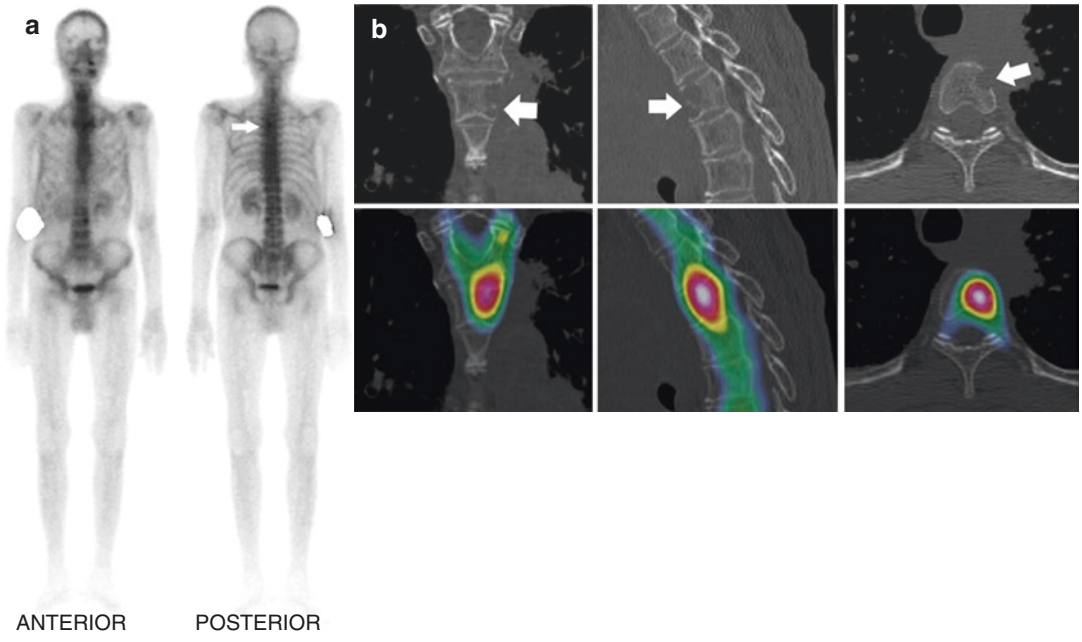

Fig. 8.22 (**a**, **b**) Known lung carcinoma in a 68-year-old male, whole-body bone scan (**a**) shows doubtful focus of uptake in the region of left sternoclavicular joint. On SPECT-CT (**b**), the uptake localizes to lytic changes in the thoracic vertebra due to local infiltration of the left lung mass (arrows)

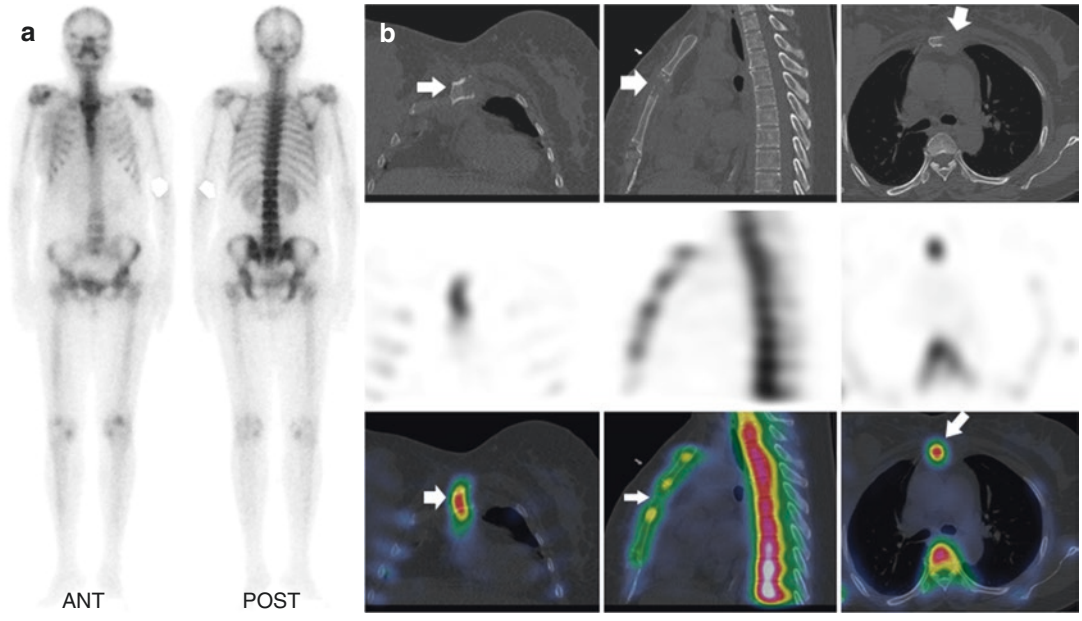

Fig. 8.23 (**a**, **b**) Forty-six-year-old female with known breast carcinoma shows mild heterogeneous uptake at the manubriosternal joint region on whole-body scan (**a**). SPECT-CT of sternum demonstrates focal lytic lesion with soft-tissue component just below manubriosternal joint suggestive of metastasis

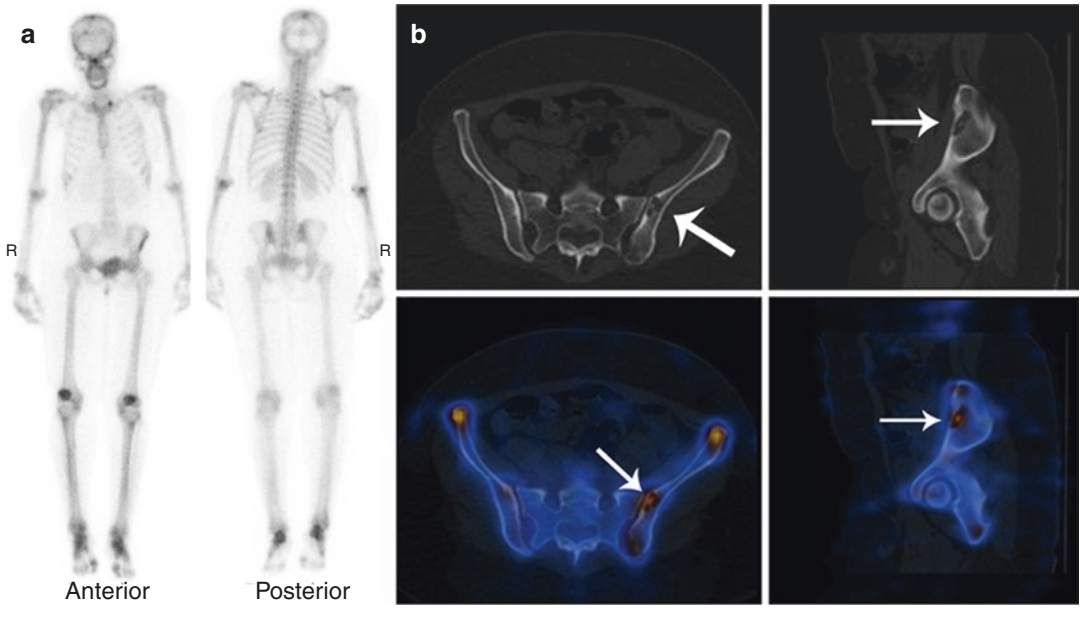

Fig. 8.24 (**a**, **b**) Whole-body bone scan (**a**) of a patient referred for metastatic evaluation shows increased tracer uptake in the knees, ankles and feet suggestive of degenerative changes. On planar imaging, no abnormal tracer uptake is seen anywhere in the skeleton to suggest metastasis. However, SPECT-CT of the pelvis (**b**) demonstrates mild tracer uptake in the left iliac bone showing two lytic lesions (arrows) suggestive of metastatic disease

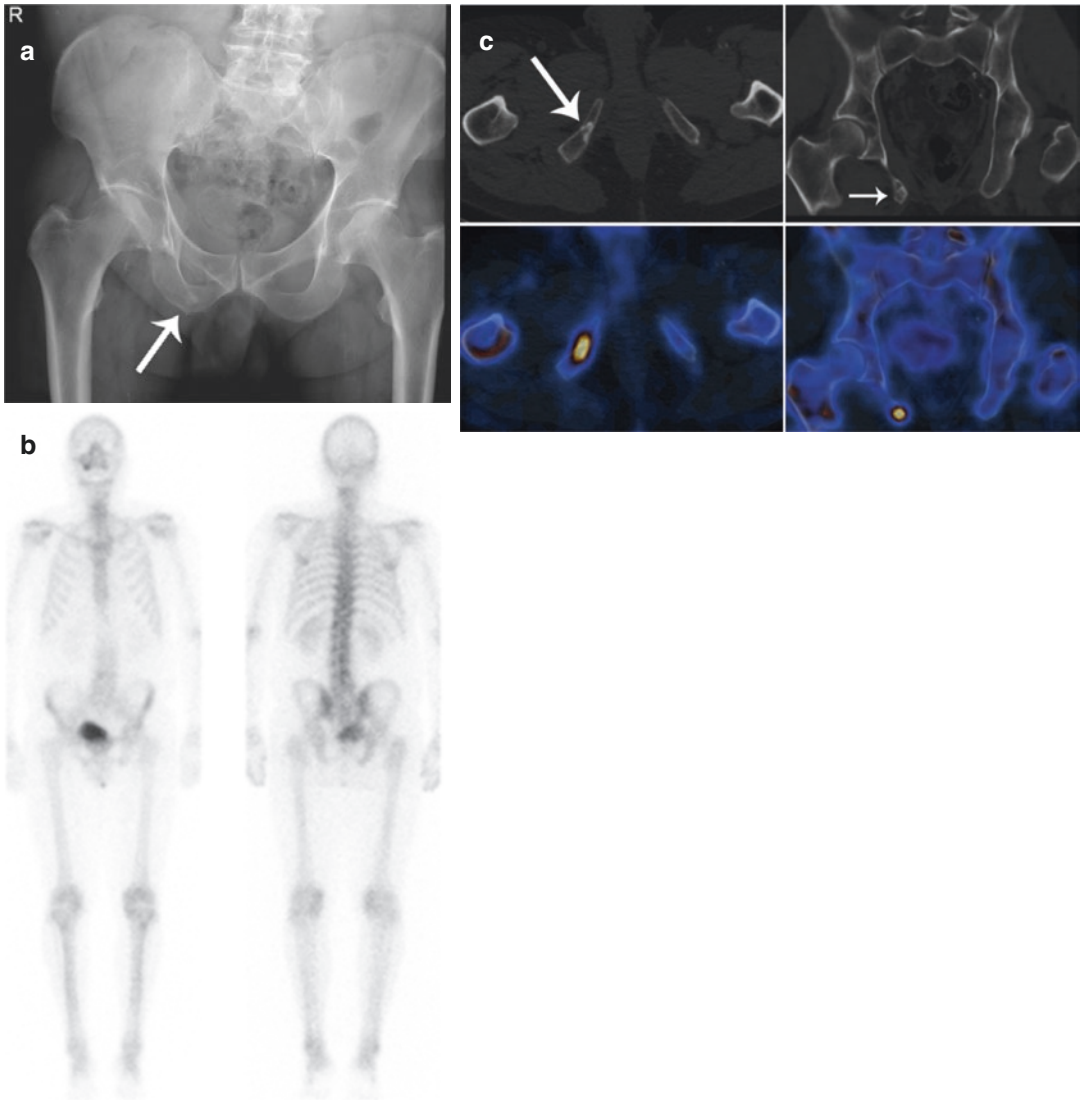

Fig. 8.25 (**a**–**c**) Patient with prostate cancer. X-ray pelvis shows a sclerotic lesion in the right ischium (arrow in **a**). Bone scan was done to rule out metastasis. Whole-body bone scan (**b**) shows no abnormal tracer uptake in the pelvic bones. However, SPECT-CT of pelvis (**c**) shows mild tracer uptake in a sclerotic lesion in the right ischium (arrows), suspicious for metastasis. In this particular example, SPECT-CT has increased sensitivity compared to planar bone scan in detection of bone lesions

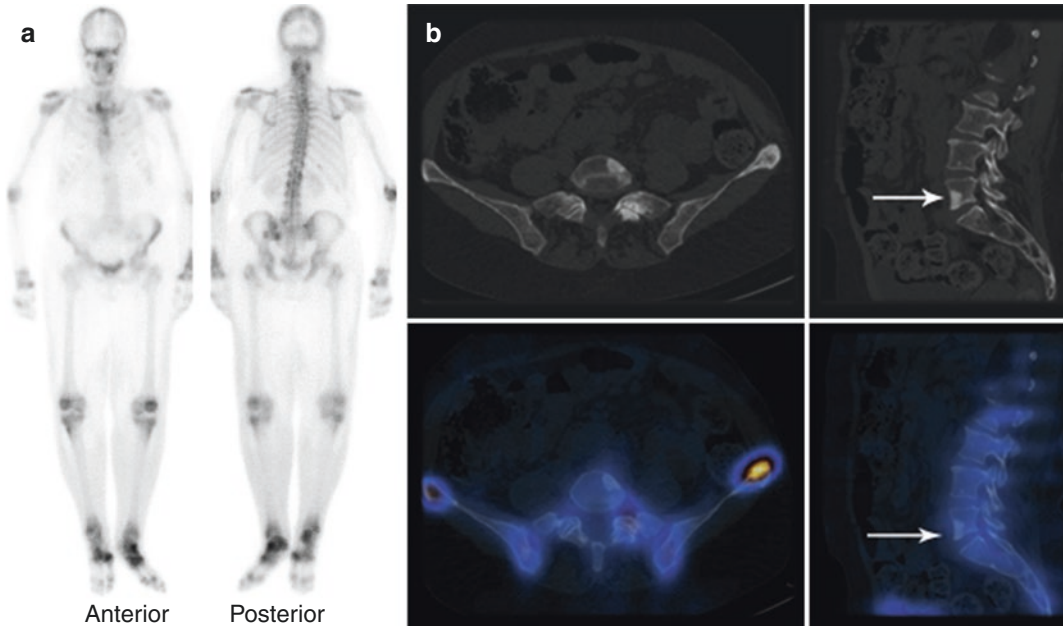

Fig. 8.26 (**a**, **b**) A patient with breast cancer underwent a bone scan with SPECT-CT for staging. The whole-body study (**a**) shows increased tracer uptake in the cervical spine, elbows, wrists, knees, ankles and feet, likely due to degenerative changes. Increased tracer uptake is seen in the sternum and left iliac bone. SPECT-CT of lumbar spine and pelvis (**b**) shows increased tracer uptake in the left iliac bone corresponding to sclerotic lesion suggestive of metastasis. Moreover, there is a sclerotic lesion in the L5 vertebral body with no tracer uptake (arrow in **b**). The findings are suggestive of bone metastases in the sternum, L5 vertebrae and left iliac bone. SPECT-CT helps in identifying metabolically inactive metastasis in this patient

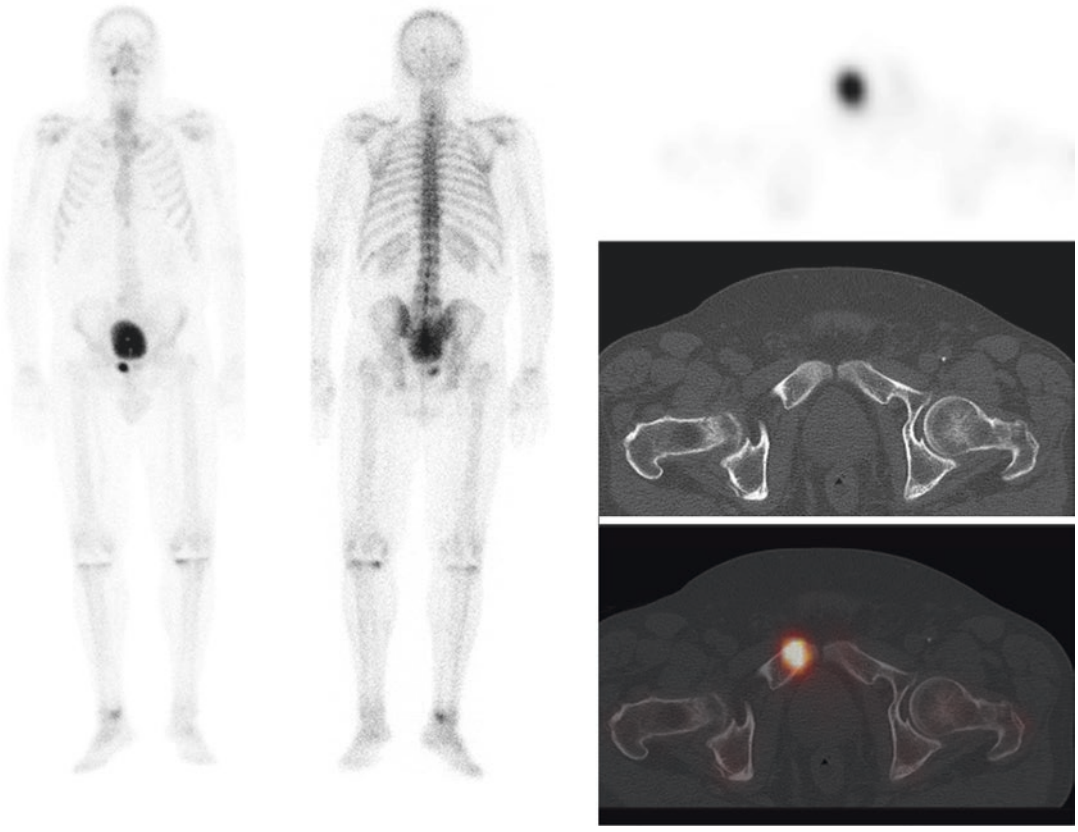

Fig. 8.27 Whole-body bone scan of a prostate cancer patient with serum PSA level 88 ng/mL shows intense focal tracer uptake at the right pubic ramus which is suspicious for metastasis, but could be due to urine contamination. Two subtle foci of tracer uptake are seen in the skull posteriorly, which is non-specific and likely benign. Note is made of bilateral knee replacement. SPECT-CT of the pelvis localizes focal uptake at the right pubic symphysis to subtle sclerosis on CT component of the study, suggestive of early bone metastasis

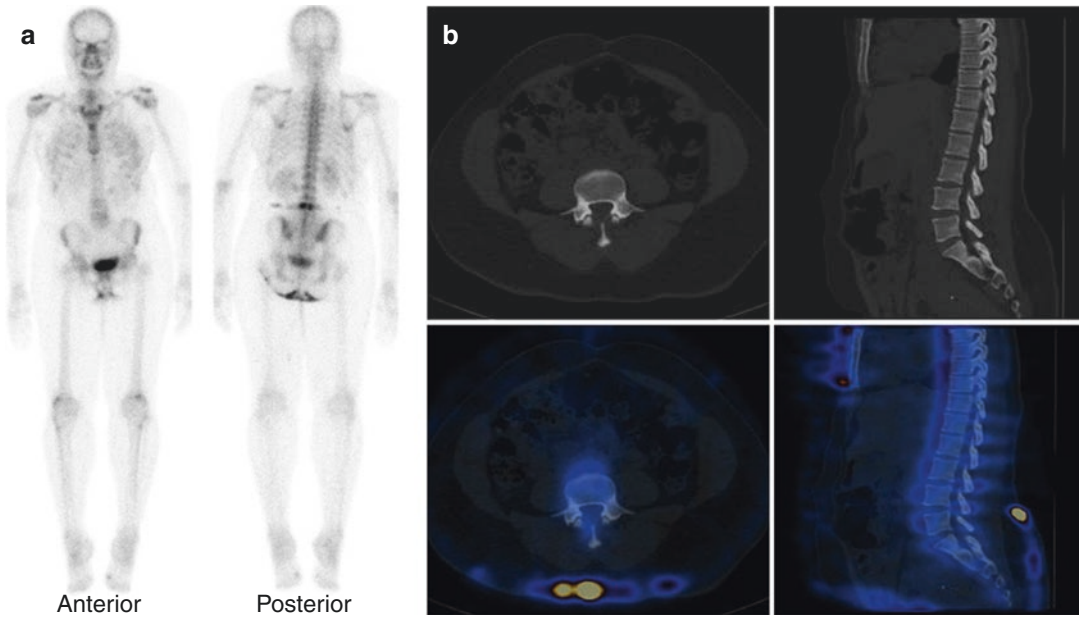

Fig. 8.28 (**a**, **b**) Breast cancer with back pain. Whole-body bone scan (**a**) shows increased tracer uptake in the region of lower lumbar vertebrae. SPECT-CT of lumbar spine (**b**) localizes the uptake to skin contamination. No morphological abnormality is seen in the lumbar vertebrae

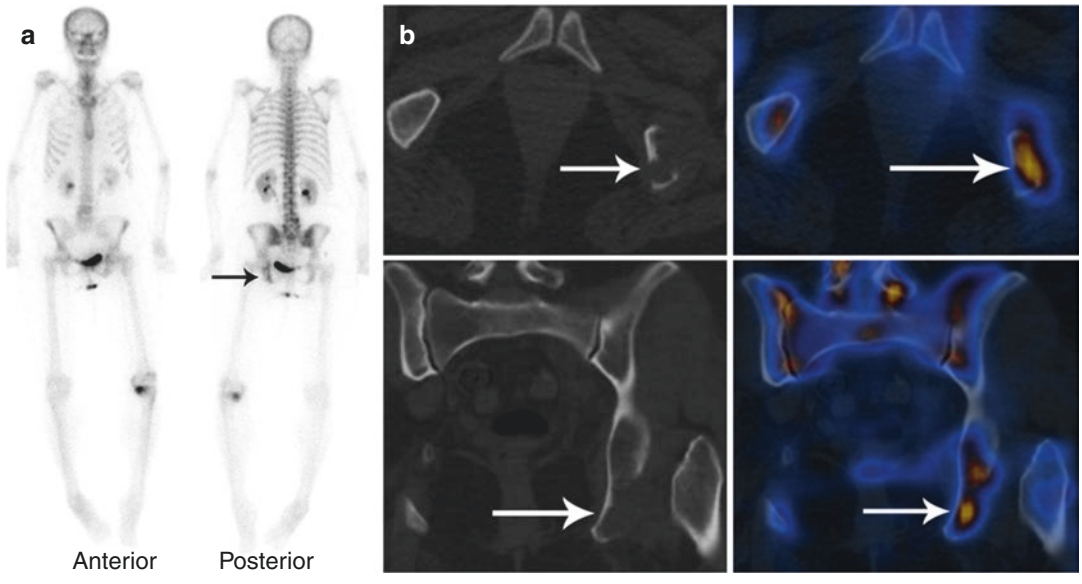

Fig. 8.29 (**a**, **b**) Patient with lung carcinoma. On whole-body bone scan (**a**), there is low-grade patchy uptake of tracer in the left ischium (arrow). This is equivocal for a skeletal metastasis. SPECT-CT of pelvis (**b**) localizes tracer uptake in the left ischium to a lytic lesion with soft-tissue component suggestive of metastasis. Further increased tracer uptake in the left knee (**a**) localizes to a lytic lesion in the medial aspect of the left tibial plateau with soft-tissue component (not shown). In this particular case, SPECT-CT was useful in increasing the confidence of the scan reader

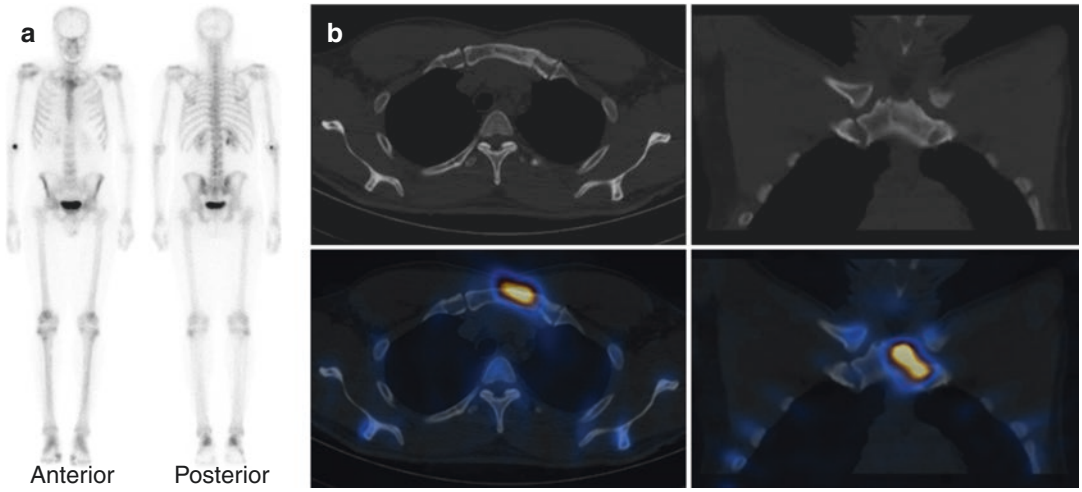

Fig. 8.30 (**a**, **b**) Prostate cancer on hormonal treatment. Increased tracer uptake is seen in the manubrio sternum on whole-body bone scan (**a**), which is not typical for metastasis. However, SPECT-CT (**b**) localizes the tracer uptake to sclerosis on CT component of the study. Although, the appearances are non-specific on planar study, it is strongly suspicious for metastasis on SPECT-CT study

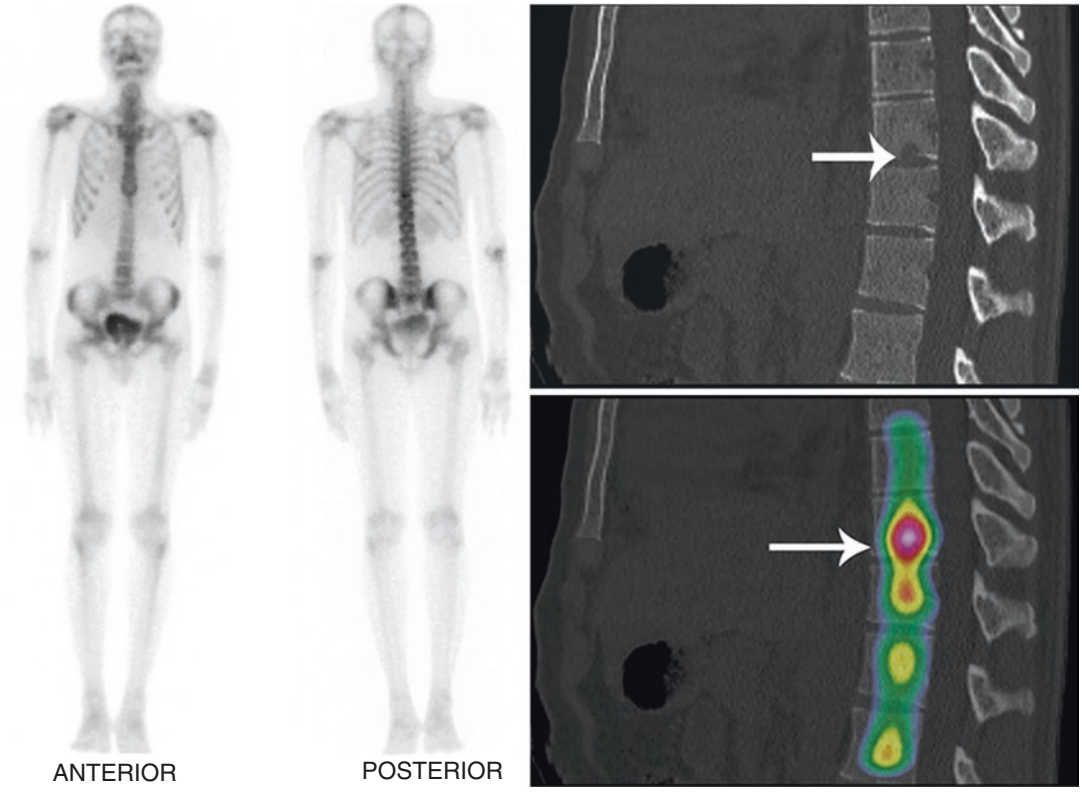

Fig. 8.31 Known lung carcinoma, whole-body bone scan shows solitary minimal increased osteoblastic activity in D10 vertebral region on whole-body study posterior view which could be metastasis but needs further anatomical correlation. The uptake localizes to a small lytic lesion in D10 vertebral body on SPECT-CT confirming metastasis (arrows)

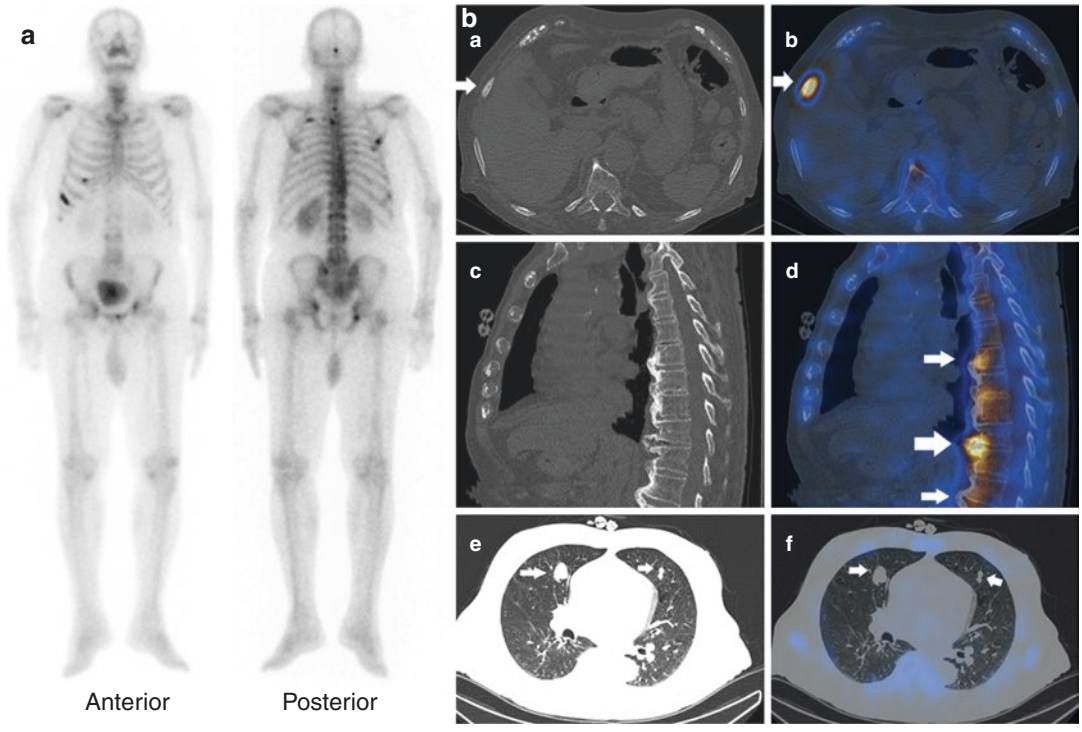

Fig. 8.32 (**a**, **b**) Sixty-year-old male patient with known prostate carcinoma shows multifocal uptake in the pelvis and thorax, and heterogeneous tracer uptake in the vertebrae (**a**). On SPECT-CT of thorax (**b**), the uptake in rib localizes to sclerotic lesion (a, b) suggestive of metastases, and uptake in vertebrae localizes to degenerative osteophytic changes (c, d). Moreover, there is incidental lung nodules on low-dose CT component of SPECT-CT (e, f), which could be metastatic and needs further evaluation

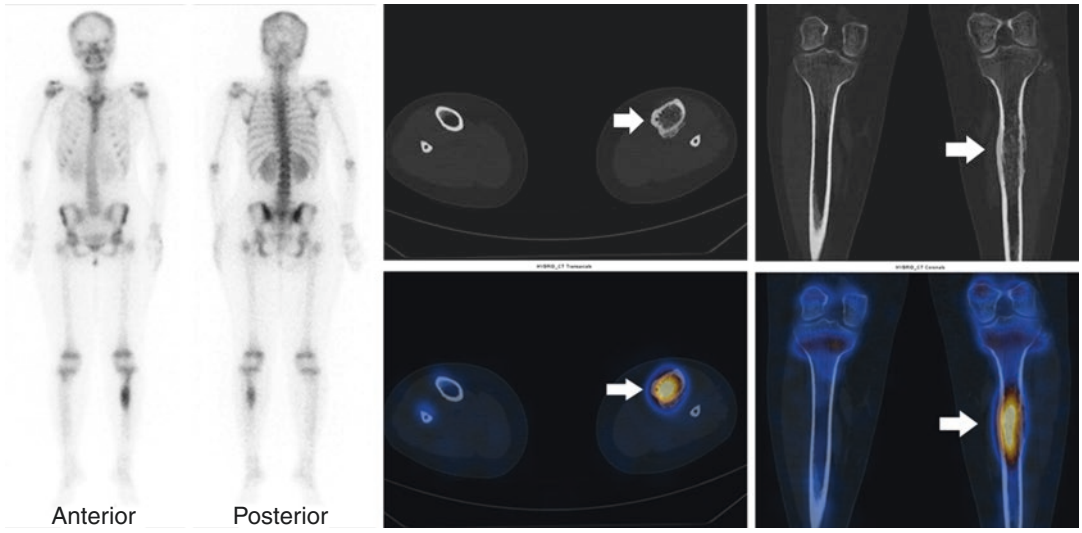

Fig. 8.33 A known case of left tibial Ewing's sarcoma, whole-body bone scan shows increased osteoblastic activity in the proximal left tibia possibly extension up to the proximal epiphysis. However, SPECT-CT localizes the uptake to intramedullary sclerosis with thick periosteal reaction (arrows) in the proximal diaphysis sparing the epiphysis and metaphysis, which is helpful in knee preserving surgery

References

1. Saha GB, editor. Fundamentals of nuclear pharmacy. 5th ed. New York: Springer; 2004.
2. Donohoe KJ, Brown ML, Collier BD, et al. Society of Nuclear Medicine procedure guideline for bone scintigraphy. Society of Nuclear Medicine website. Accepted 20 Jun 2003.
3. Van den Wyngaert T, Strobel K, Kampen WU, Kuwert T, van der Bruggen W, Mohan HK, Gnanasegaran G, Delgado-Bolton R, Weber WA, Beheshti M, Langsteger W, Giammarile F, Mottaghy FM, Paycha F, EANM Bone & Joint Committee and the Oncology Committee. The EANM practice guidelines for bone scintigraphy. Eur J Nucl Med Mol Imaging. 2016;43(9):1723–38.
4. Gnanasegaran G, Barwick T, Adamson K, Mohan H, Sharp D, Fogelman I. Multislice SPECT/CT in benign and malignant bone disease: when the ordinary turns into the extraordinary. Semin Nucl Med. 2009;39(6):431–42.
5. Kuwert T. Skeletal SPECT/CT: a review. Clin Transl Imaging. 2014;2:505–17.
6. Poon M, Zeng L, Zhang L, Lam H, Emmenegger U, Wong E, et al. Incidence of skeletal-related events over time from solid tumour bone metastases reported in randomised trials using bone-modifying agents. Clin Oncol (R Coll Radiol). 2013;25(7):435–44.
7. Melton LJ III, Kyle RA, Achenbach SJ, Oberg AL, Rajkumar SV. Fracture risk with multiple myeloma: a population-based study. J Bone Miner Res. 2005;20(3):487–93.
8. Hofbauer LC, Rachner TD, Coleman RE, Jakob F. Endocrine aspects of bone metastases. Lancet Diabetes Endocrinol. 2014;2(6):500–12.
9. Fogelman I, Cook G, Israel O, Van der Wall H. Positron emission tomography and bone metastases. Semin Nucl Med. 2005;35(2):135–42.
10. Coleman RE, Mashiter G, Whitaker KB, Moss DW, Rubens RD, Fogelman I. Bone scan flare predicts successful systemic therapy for bone metastases. J Nucl Med. 1988;29(8):1354–9.
11. Rosenthal DI. Radiologic diagnosis of bone metastases. Cancer. 1997;80(8 Suppl):1595–607.
12. Gutzeit A, Doert A, Froehlich JM, Eckhardt BP, Meili A, Scherr P, et al. Comparison of diffusion-weighted whole body MRI and skeletal scintigraphy for the detection of bone metastases in patients with prostate or breast carcinoma. Skelet Radiol. 2010;39(4):333–43.
13. Takenaka D, Ohno Y, Matsumoto K, Aoyama N, Onishi Y, Koyama H, et al. Detection of bone metastases in non-small cell lung cancer patients: comparison of whole-body diffusion-weighted imaging (DWI), whole-body MR imaging without and with DWI, whole-body FDG-PET/CT, and bone scintigraphy. J Magn Reson Imaging. 2009;30(2):298–308.
14. Davila D, Antoniou A, Chaudhry MA. Evaluation of osseous metastasis in bone scintigraphy. Semin Nucl Med. 2015;45:3–15.
15. Azad GK, Taylor B, Rubello D, Colletti PM, Goh V, Cook GJ. Molecular and functional imaging of bone metastases in breast and prostate cancers: an overview. Clin Nucl Med. 2016;41:e44–50.
16. Cook GJ, Azad GK, Goh V. Imaging bone metastases in breast cancer: staging and response assessment. J Nucl Med. 2016;57(Suppl 1):27s–33s.
17. Agrawal K, Marafi F, Gnanasegaran G, Van der Wall H, Fogelman I. Pitfalls and limitations of radionuclide planar and hybrid bone imaging. Semin Nucl Med. 2015;45(5):347–72.
18. Israel O, Pellet O, Biassoni L, De Palma D, Estrada-Lobato E, Gnanasegaran G, Kuwert T, la Fougère C, Mariani G, Massalha S, Paez D, Giammarile F. Two decades of SPECT/CT - the coming of age of a technology: an updated review of literature evidence. Eur J Nucl Med Mol Imaging. 2019;46(10):1990–2012.
19. Gnanasegaran G, Cook G, Adamson K, Fogelman I. Patterns, variants, artifacts, and pitfalls in conventional radionuclide bone imaging and SPECT/CT. Semin Nucl Med. 2009;39(6):380–95.
20. Mohd Rohani MF, Zanial AZ, Suppiah S, Phay Phay K, Mohamed Aslum Khan F, Mohamad Najib FH, Mohd Noor N, Arumugam M, Amir Hassan SZ, Vinjamuri S. Bone single-photon emission computed tomography/computed tomography in cancer care in the past decade: a systematic review and meta-analysis as well as recommendations for further work. Nucl Med Commun. 2021;42(1):9–20.
21. Gayed IW, Kim EE, Awad J, Joseph U, Wan D, John S. The value of fused SPECT/CT in the evaluation of solitary skull lesion. Clin Nucl Med. 2011;36:538–41.
22. Sharma P, Kumar R, Singh H, Bal C, Julka PK, Thulkar S, Malhotra A. Indeterminate lesions on planar bone scintigraphy in lung cancer patients: SPECT, CT or SPECT-CT? Skelet Radiol. 2012;41:843–50.
23. Sharma P, Singh H, Kumar R, Bal C, Thulkar S, Seenu V, Malhotra A. Bone scintigraphy in breast cancer: added value of hybrid SPECT-CT and its impact on patient management. Nucl Med Commun. 2012;33:139–47.
24. Sharma P, Jain TK, Reddy RM, Faizi NA, Bal C, Malhotra A, Kumar R. Comparison of single photon emission computed tomography-computed tomography, computed tomography, single photon emission computed tomography and planar scintigraphy for characterization of isolated skull lesions seen on bone scintigraphy in cancer patients. Indian J Nucl Med. 2014;29:22–9.
25. Rager O, Lee-Felker SA, Tabouret-Viaud C, Felker ER, Poncet A, Amzalag G, et al. Accuracy of whole-body HDP SPECT/CT, FDG PET/CT, and their combination for detecting bone metastases in breast cancer: an intrapersonal comparison. Am J Nucl Med Mol Imaging. 2018;8:159–68.
26. Zhang Y, Li B, Wu B, Yu H, Song J, Xiu Y, Shi H. Diagnostic performance of whole-body bone scintigraphy in combination with SPECT/CT for detection of bone metastases. Ann Nucl Med. 2020;34:549–58.

27. Palmedo H, Marx C, Ebert A, Kreft B, Ko Y, Türler A, et al. Whole-body SPECT/CT for bone scintigraphy: diagnostic value and effect on patient management in oncological patients. Eur J Nucl Med Mol Imaging. 2014;41:59–67.
28. Fonager RF, Zacho HD, Langkilde NC, Fledelius J, Ejlersen JA, Haarmark C, et al. Diagnostic test accuracy study of 18F-sodium fluoride PET/CT, 99mTc-labelled diphosphonate SPECT/CT, and planar bone scintigraphy for diagnosis of bone metastases in newly diagnosed, high-risk prostate cancer. Am J Nucl Med Mol Imaging. 2017;7:218–27.
29. Teyateeti A, Tocharoenchai C, Muangsomboon K, Komoltri C, Pusuwan P. A comparison of accuracy of planar and evolution SPECT/CT bone imaging in differentiating benign from metastatic bone lesions. J Med Assoc Thail. 2017;100:100–10.
30. Fleury V, Ferrer L, Colombié M, Rusu D, Le Thiec M, Kraeber-Bodéré F, et al. Advantages of systematic trunk SPECT/CT to planar bone scan (PBS) in more than 300 patients with breast or prostate cancer. Oncotarget. 2018;9:31744–52.
31. Mavriopoulou E, Zampakis P, Smpiliri E, Spyridonidis T, Rapti E, Haberkorn U, et al. Whole body bone SPET/CT can successfully replace the conventional bone scan in breast cancer patients. A prospective study of 257 patients. Hell J Nucl Med. 2018;21:125–33.
32. de Leiris N, Leenhardt J, Boussat B, Montemagno C, Seiller A, Phan Sy O, et al. Does whole-body bone SPECT/CT provide additional diagnostic information over [18F]-FCH PET/CT for the detection of bone metastases in the setting of prostate cancer biochemical recurrence? Cancer Imaging. 2020;20:58.
33. Rager O, Nkoulou R, Exquis N, Garibotto V, Tabouret-Viaud C, Zaidi H, et al. Whole-body SPECT/CT versus planar bone scan with targeted SPECT/CT for metastatic workup. BioMed Res Intern. 2017;2017:7039406.
34. Guezennec C, Keromnes N, Robin P, Abgral R, Bourhis D, Querellou S, et al. Incremental diagnostic utility of systematic double-bed SPECT/CT for bone scintigraphy in initial staging of cancer patients. Cancer Imaging. 2017;17:16.
35. Abikhzer G, Gourevich K, Kagna O, Israel O, Frenkel A, Keidar Z. Whole-body bone SPECT in breast cancer patients: the future bone scan protocol? Nucl Med Commun. 2016;37:247–53.
36. Tuncel M, Lay Ergun E, Caglar Tuncali M. Clinical impact of SPECT-CT on bone scintigraphy in oncology: pattern approach. J BUON. 2016;21(5):1296–306.